Structure-reactivity relationships on substrates and inhibitors of the lysine deacylase Sirtuin 2 from *Schistosoma mansoni* (*Sm*Sirt2)

Daria Monaldi[1], Dante Rotili[2*], Julien Lancelot[3], Martin Marek[4], Alessia Lucidi[2], Daniela Tomaselli[2], Elizabeth Ramos-Morales[4], Christophe Romier[4], Raymond J. Pierce[3], Antonello Mai[2*] and Manfred Jung[1*]

[1]Institute of Pharmaceutical Sciences, University of Freiburg, Albertstr. 25, 79104, Freiburg, Germany.

[2]Dipartimento di Chimica e Tecnologie del Farmaco "Sapienza" Università di Roma, 00185 Rome, Italy

[3]Université de Lille, CNRS, Inserm, CHU Lille, Institut Pasteur de Lille, U1019 - UMR 8204 - CIIL - Centre d'Infection et d'Immunité de Lille, 59000 Lille, France

[4]Département de Biologie Structurale Intégrative, Institut de Génétique et Biologie Moléculaire et Cellulaire (IGBMC), Université de Strasbourg (UDS), CNRS, INSERM, 67404 Illkirch Cedex, France

* corresponding authors, E-mail : dante.rotili@uniroma1.it, antonello.mai@uniroma1.it, manfred.jung@pharmazie.uni-freiburg.de

ABSTRACT

The standard drug for treatment of the neglected disease Schistosomiasis is Praziquantel, and the possible emergence of resistance to this treatment makes the research on novel therapeutic agents necessary and urgent. To this end, the targeting of *Schistosoma mansoni* epigenetic enzymes, which regulate the parasitic life cycle, emerged as promising approach. Due to strong effects of human Sirtuin inhibitors on parasite survival and reproduction, *Schistosoma* sirtuins were postulated as potential therapeutic targets. *In vitro* testing of synthetic substrates of *Sm*Sirt2 and kinetic experiments on a myristoylated peptide newly demonstrated lysine long chain deacylation as an intrinsic *Sm*Sirt2 activity in addition to the known deacetylation. Focused *in vitro* screening of the GSK Kinetobox library and structure-activity relationships (SAR) of identified hits, led to the first *Sm*Sirt2 inhibitors with activity in the low micromolar range. Several *Sm*Sirt2 inhibitors showed potency against both larval schistosomes (viability) and adult worms (pairing, egg laying) in culture without general toxicity to human cancer cells.

INTRODUCTION

Schistosomiasis is a neglected tropical disease, affecting millions of people in tropical and sub-tropical countries and causing more than 300000 deaths per year.[1] One of its major causative agents is the blood fluke *Schistosoma mansoni*, characterized by a complex life cycle, where the parasite is converted into four morphologically distinct forms, with two of them, schistosomula and adult worms, present in the final human host. Praziquantel is so far the gold standard for the treatment of schistosomiasis, showing several positive features like low cost, high efficacy and low toxicity,[2] that made possible its use for mass treatment campaigns.[3] The long term mass treatment with Praziquantel has led to a reduction in mortality and morbidity in endemic areas,[4,5] but also to a reduction in treatment efficacy and, in some cases, the isolation of resistant strains.[6,7,8,9] This aspect, in association with the drug inactivity on larval stages and its unknown mechanism of action,[2,7] render relying on only one drug inadequate in the long term and highlights the need for the development of novel therapeutic agents. Different approaches have been already studied, for example the use of artemisinins[10] and benzodiazepines,[11] but none of them is similar to Praziquantel in terms of efficacy, safety and cost.

The publication of the *Schistosoma mansoni* genome sequence[12] made the research and validation of novel therapeutic targets a particularly promising paradigm for the development of novel antischistosomal drugs. A drug repurposing approach,[13] based on targeting orthologues of proteins already targeted in other pathologies,[10] has demonstrated potential for developing compounds able to selectively inhibit parasitic enzymes without affecting the correspondent human isoforms. Moreover, since schistosomes can be considered similar to cancer cells in terms of intensive metabolic activity and invisibility to host immune system,[14] our interest is focused on histone deacetylase enzymes (HDACs), which are able to remove acetyl groups from lysine residues of histones and other proteins and are already known cancer drug targets with clinically

approved drugs. Such HDAC inhibitors and also development candidates are able to selectively arrest cancer cells growth without affecting normal cells.[15,16,17] The essentiality of several histone deacetylases for growth and survival has already been demonstrated in a variety of parasite genera, including *Plasmodium*, *Leishmania*, *Trypanosoma* and *Schistosoma*.[18] The complex life cycles of these parasites are subject to complex epigenetic regulation and the selective inhibition of enzymes involved in these processes, including HDACs, represents a valid therapeutic strategy. For example, in the cases of *Plasmodium falciparum* and *Trypanosoma brucei* several molecules display selective *in vitro* and *in vivo* inhibitory activity against parasitic Zn^{2+}-dependent HDACs (class I and II).[18] This approach has also led to the development of selective inhibitors of *S. mansoni* HDAC8, including a mercaptoacetamide analogue of suberoylanilide hydroxamic acid (SAHA),[19] alkylhydroxamates[20] and benzoylhydroxamates,[21] characterized by submicro or nanomolar IC_{50} values for *Sm*HDAC8 with good selectivity over hHDAC1, hHDAC6 and, in some cases, also over hHDAC8. Some of these compounds had also low micromolar EC_{50} values for killing schistosome larvae and abolish pairing stability and egg laying in adult worms.[19-21]

The situation is different for NAD^+-dependent HDACs (class III, Sirtuins), where, despite their evident potential as human anticancer and metabolic disease targets,[22] only one compound (Selisistat) has reached clinical trials so far as a potential treatment for Huntington´s disease. In parasites, sirtuin isoforms have been identified in *Plasmodium falciparum* (*Pf*Sir2A and *Pf*Sir2B),[23,24] in *Trypanosoma cruzi* (*Tc*Sir2rp1 and *Tc*Sir2rp3)[25,26] and in *Leishmania* (*Lm*Sir2rp1 and *Li*sir2rp1)[27,28] but most *in vitro* tested inhibitors showed modest activity and/or lack of selectivity.[18] An exception is provided by bisnaphthalimidopropyl derivatives that showed significant activity *in vitro* and in mice chronically infected with *Leishmania infantum*.[29]

In 2013 Lancelot *et al.* published the identification and characterisation of five *Schistosoma mansoni* sirtuins (*Sm*Sirt1, *Sm*Sirt2, *Sm*Sirt5, *Sm*Sirt6 and *Sm*Sirt7) as orthologues of their respective mammalian counterpart isoforms.[30] Furthermore, it was demonstrated that Sirtinol and Salermide, known inhibitors of hSirt1 and hSirt2,[31,32,33] in addition to be inducers of selective apoptosis in cancer cell lines,[32,34] and to show protective effects in a muscular dystrophy model in nematodes,[35] have pro-apoptotic effects in schistosome larvae (schistosomula), through DNA fragmentation, and markedly reduce pairing stability and egg production in adult worms. These features support the potential of *Schistosoma* sirtuins as drug targets for the development of novel and selective antischisosomal drugs.

Beyond the deacetylase activity, human sirtuins are also implicated in the removal of short, medium and long fatty acyl groups from lysine residues of histones and non-histones proteins.[36,37,38,39,40,41,42] Lysine acylation has been identified as a posttranslational modification and it is strongly connected to regulation of metabolism. In fact, metabolic intermediates are used for this process and enzymes implicated in energy pathways are, in many cases, subject to these modifications.[39,43,44] Although deacylation of acyllysine is a common feature for all mammalian sirtuins, they show a difference in specificity and efficiency in the catalysis of this process that is typical for each isoform and may be quite distinct from their deacetylase activity.[45] In parasites, studies regarding lysine deacylation are lacking so far with the exception of the medium and long fatty acyl chain removal by P*f*Sir2A in *Plasmodium falciparum*.[46] In a previous study, we established a homogeneous in vitro assay for the determination of *Sm*Sirt2 deacetylase activity which, using the readily available Z-(Ac)Lys-AMC (ZMAL, **1**), represents an optimal tool for cost efficient high throughput campaigns.[47] In order to further characterize the function of *Sm*Sirt2, we performed and report here the analysis of *Sm*Sirt2 lysine deacylation activity by the use of both lysine-derived small molecule and oligopeptidic substrates.

Moreover, with the aim of finding novel and selective drug-like inhibitors of *Sm*Sirt2, we present an extensive structure-activity relationship study concerning novel hits identified by an *in vitro* screening of the Kinetobox library,[48] provided by GSK. This library is constituted by compounds which were shown to be potent and specific inhibitors of growth of *Leishmania donovani*, *Trypanosoma cruzi* and *Trypanosoma brucei* with low human cellular cytotoxicity.[48] The kinetoplastid parasites *Leishmania sp.* and *Trypanosoma sp.* are characterized by complex morphological changes and an involvement of epigenetic regulation during their life cycle, and we postulated that the screening of this diverse library would be a good starting point for our study on *S. mansoni* aimed at identifying novel chemical entities able to interfere with the parasite growth. *S. mansoni* is phylogenetically quite different from kinetoplastides, but has similar dynamic phenotypic changes through the different life stages, some of them implying epigenetic modifications.[49] This inhibitor collection is freely available and provides a set of 592 compounds with diverse structural features, potentially providing novel chemical space for chemically yet uncharted targets. Here we present new hits for *Sm*Sirt2 (as well as hSirt2) and present initial SAR to further characterize ligand affinity and specificity to *Sm*Sirt2. In particular, we can show for the first time that *Sm*Sirt2 is a druggable target with selectivity over hSirtuin 2. Moreover, several of the characterized *Sm*Sirt2 inhibitors were active against both schistosomula larvae and adult worms in culture. Some of the negative controls showed activity on *Schistosoma* as well, but they were also toxic against human cancer cells in culture. In contrast, selective *Sm*Sirt2 inhibitors did not show toxicity in mammalian cells, further supporting the use of *Sm*Sirt2 as a valuable drug target in schistosomes.

RESULTS AND DISCUSSION

Short-, medium-, and long-chain deacylation activity of *Sm*Sirt2. To extend the biochemical characterization of *Sm*Sirt2 activity, we studied its ability to deacylate long chain fatty acids from the ε-amino group of lysine substrates. We synthesized seven analogues of the *Sm*Sirt2 substrate ZMAL (Z-(Ac)Lys-AMC) **1**, ie **3a** (Z-(But)Lys-AMC), **3b** (Z-(Hex)Lys-AMC), **3c** (Z-(Oct)Lys-AMC), **3d** (Z-(Dec)Lys-AMC), **3e** (Z-(Lau)Lys-AMC), **3f** (Z-(Myr)Lys-AMC) and **3g** (Z-(Pal)Lys-AMC), by replacing its acetyl group with short, medium and long acyl chains. The substrate **1** was synthesized according to published procedures.[50] For the preparation of **3a-g**, the appropriate acyl chlorides (commercially available for **3a-d**,**g**, and synthesized for **3e** and **3f** by reaction of the corresponding lauric or myristic acid with thionyl chloride) were treated with Z-Lys-OH leading to the formation of the ε-acyl-Z-Lys-OH **2a-g**, which were converted into the desired substrates **3a-g** by treatment with phosphorus oxychloride and 7-amino-4-methylcoumarin (AMC) (**Scheme 1**).

Scheme 1. Synthesis of 3a-g[a]

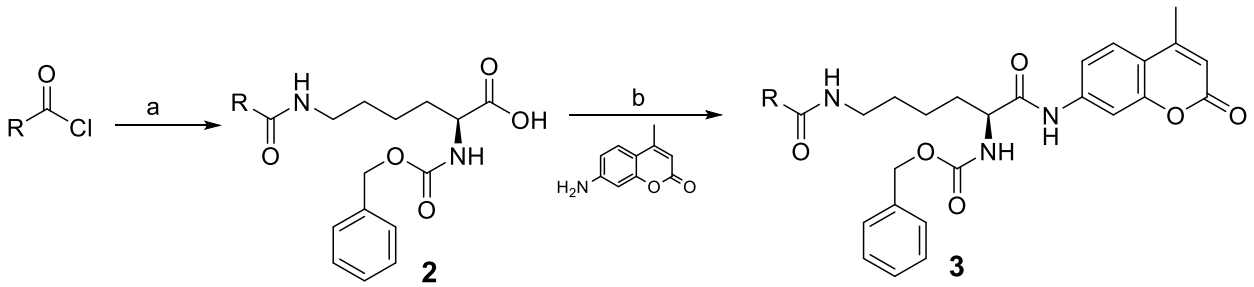

R = $(CH_2)_2CH_3$ (**a**), $(CH_2)_4CH_3$ (**b**), $(CH_2)_6CH_3$ (**c**), $(CH_2)_8CH_3$ (**d**), $(CH2)_{10}CH_3$ (**e**), $(CH_2)_{12}CH_3$ (**f**), $(CH_2)_{14}CH_3$ (**g**)

[a]Reagents and conditions: a) Z-Lys-OH, 1 M sodium hydroxide, water, rt, 20-45 min; b) AMC (structure shown), phosphoryl chloride, dry pyridine, -15 ^{0}C, 40 min to 3h.

Then we used the acyl-lysine substrates **3a-g**, in comparison to the acetylated **1**, in the homogeneous fluorescence based assay,[47] in order to evaluate the ability of *Sm*Sirt2 to catalyse their conversion into free lysine substrate. Compounds **1**, **3a-g** have been tested at 10.5 µM with one time point measurement, according to a published procedure for **1**.[47] As shown in Figure 1A (Table S1 in Supporting Information), the measured substrate conversion increases with increasing chain length from acetyl to hexanoyl analogues (see **1**, **3a** and **3b**), then exhibit an opposite trend from the octanoyl to the palmitoyl analogue (from **3c** to **3g**). When tested with hSirt2 (Figure 1B, Table S2), **1** and **3a-g** showed a somewhat discontinuous pattern of conversion, with **3a** (butyryl) and **3b** (hexanoyl) as the best substrates. Unfortunately, solubility issues did not allow the measurement of K_m values for any of the ZMAL analogues in order to obtain a more quantitative overview. But we performed a quantitative analysis on peptidic substrates (see below).

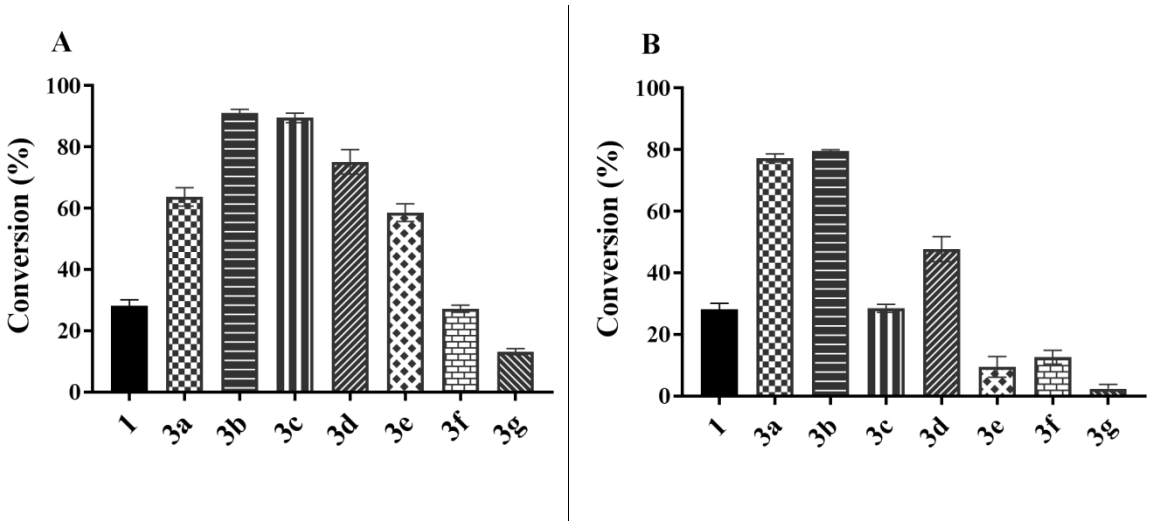

Figure 1. In vitro conversion of **1** (acetyl) and **3a-g** (see Scheme 1) by *Sm*Sirt2 (**A**) and hSirt2 (**B**). A pure AMC sample is measured to simulate a (hypothetical) conversion of 100% for comparison. Errors are represented as standard deviation of the mean (SD, n=3).

Nicotinamide (NA) is a physiological sirtuin inhibitor which, once released from NAD^+, stays in a subpocket of the enzyme (pocket C) and, by a rebound mechanism, can block the enzymatic activity.[51] In hSirt2 the lysine acyl chain pocket is in a close contact with the C pocket, determining the possibility for the NA potency to be influenced by the substrate acyl chain length.[37] To study the effect of short-, medium- and long-chain lysine substrates on the relative NA potency for *Sm*Sirt2 inhibition, we measured IC_{50} values for NA in presence of our ZMAL analogues **1**, **3a**-**g**. As shown in Figure 2 (Table S3), the IC_{50} values of NA are similar using the acetylated **1** to the octanoyl substrate **3c**, after which it increases with the growth of the acyl chain length. Since an opposite trend has been published for acylated peptides and hSirt2,[37] we can hypothesize that, despite the structural homology between the parasitic and the hSirt2, these two enzymes are characterized by different kinetics.

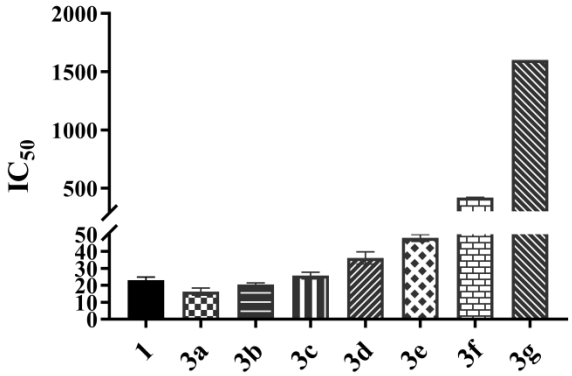

Figure 2. IC_{50} values of NA against *Sm*Sirt2 in the presence of the acetylated substrate **1** and the acylated ZMAL analogues **3a-g** (see Scheme 1). Errors are represented as standard error of the mean (SEM, n=3). IC_{50} values are reported in Table S3 (Supporting information).

In order to gain a more quantitative insight into the interplay between *Sm*Sirt2 and its acylated substrates, we performed a kinetic analysis through the use of a HPLC-based assay using more

soluble peptides, not tagged with a fluorescent label to rule out potential artifactual effects. K_m, k_{cat} and k_{cat}/K_m of *Sm*Sirt2 were measured in the presence of an acetylated (PSDKac) and a myristoylated peptide (PSDKmyr) derived from α-tubulin. As shown in Figure 3, the acyl chain elongation in PSDKmyr determined an increase of affinity for *Sm*Sirt2 without affecting the enzymatic turnover, with consequent threefold higher catalytic efficiency in the presence of PSDKmyr than with PSDKac (Table 1). Interestingly, these results are in accordance with the conversion of **1** and **3f** measured by the homogeneous fluorescent based assay described before (Figure 1A, Table S1).

Moreover, since in hSirt2 the acylated substrate binds the enzyme before NAD^+,[52] the length of the acyl group could influence the NAD^+ binding affinity for *Sm*Sirt2 and have, more generally, an influence on the NAD^+ reaction. Consequently, the K_m values of NAD^+ were also analysed in the presence of PSDKac and PSDKmyr, respectively. As shown in Figure 4, the extension of the peptide chain length increases the binding affinity of NAD^+ to *Sm*Sirt2 and the catalytic turnover. In fact, a threefold higher k_{cat} is the reason for a better catalytic efficiency in presence of PSDKmyr than with PSDKac (Table 1).

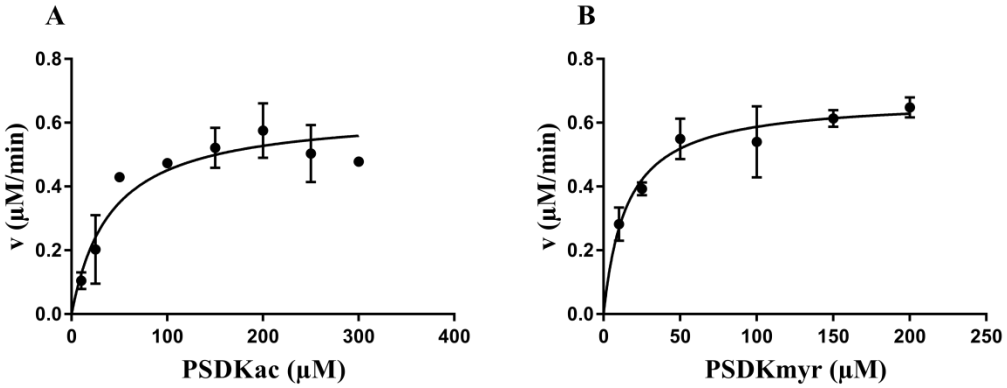

Figure 3. Michaelis-Menten plots for *Sm*Sirt2 dependent deacetylation (**A**) and demyristoylation (**B**). Error bars indicate standard error of the mean ($n \geq 2$).

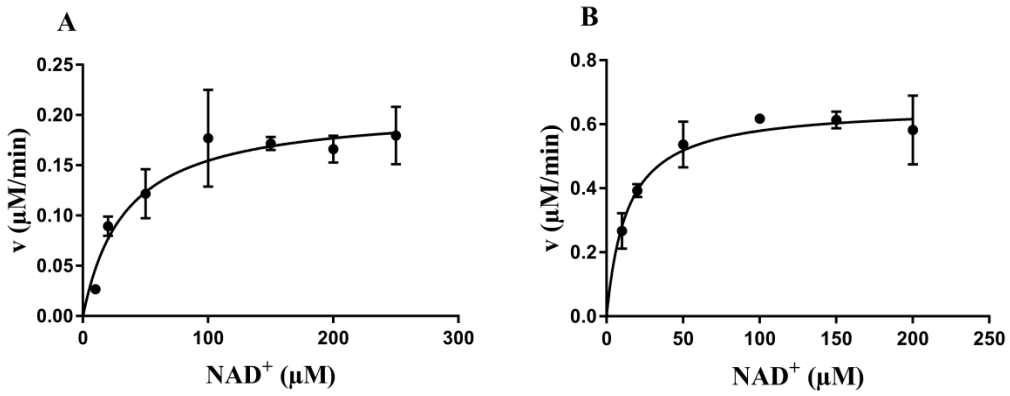

Figure 4. Michaelis-Menten plots for NAD^+ with PSDKac (**A**) and with PSDKmyr (**B**) in *Sm*Sirt2. Error bars indicate standard error of the mean ($n \geq 2$).

Table 1. Kinetic parameters for PSDKac, PSDKmyr and NAD^+ for *Sm*Sirt2.

	K_m (µM)[a]	k_{cat} (min^{-1})[a]	k_{cat}/K_m ($s^{-1}M^{-1}$)[a]
PSDKac	40.9 ± 12.2	(31.8 ± 2.4) 10^{-2}	(1.3 ± 0.3) 10^{2}
PSDKmyr	15.1 ± 2.5	(33.8 ± 1.3) 10^{-2}	(3.7 ± 0.9) 10^{2}
NAD^+ (PSDKac)	33.9 ± 8.5	(10.3 ± 0.6) 10^{-2}	(5.1 ± 1.8) 10^{1}
NAD^+ (PSDKmyr)	13.3 ± 2.3	(32.3 ± 1.3) 10^{-2}	(4.1 ± 0.9) 10^{2}

[a]Reported as ± SE.

To further characterize the deacylation reactivity, we compared the potency of selected reference hSirt2 deacetylation inhibitors (NA, SirReal1 and 2,[53] AEM2[54]) with their ability to inhibit the demyristoylation reaction. As reported in Table 2, while in hSirt2 these compounds show higher inhibitory potency for deacetylation than for demyristoylation, with the only exception of NA, they did not inhibit either reaction catalysed by *Sm*Sirt2.

Table 2. Activity of hSirt2 standard inhibitors with 1 or 3f as substrates.

Compound	*Sm*Sirt2 IC_{50} [μM][a] or % inhibition at 20 μM		hSirt2 IC_{50} [μM][a] or % inhibition at 20 μM	
	1	**3f**	**1**	**3f**
NA	23.1 ± 1.8	420 ± 1.16	49.8 ± 4.6[b]	77.0 %[c]
SirReal1	24.2 %	< 15 %	3.7[c]	< 15 %
SirReal2	< 15 %	< 15 %	0.4[c]	< 15 %
AEM2	< 15 %	< 15 %	2.5 ± 0.2[b]	42.8 %

[a]IC_{50} are reported as ± SEM (n=3). [b]Reference [55]. [c]Reference [53].

***Sm*Sirt2 inhibition.** Using the *in vitro*[56] assay described above we initially screened the FDA-approved drugs library (provided by Enzo Life Sciences (ELS) AG, Switzerland) that had already been tested on schistosomula and adult worms.[57,58] Idebenone (**4**) emerged as an overlapping compound that was known to block the growth of schistosomula, showed good *Sm*Sirt2 inhibition potency and selectivity over hSirt2[59] (Figure 5). Although Idebenone probably has a pleiotropic mode of action, this led credency to our approach to identify druggable molecules from a diverse set of compounds that also show antischistosomal activity. We next proceeded with the GSK Kinetobox library, which was initially tested at the fixed assay concentration of 25 μM. Since we were looking for compounds with an IC_{50} in the low micromolar range, we focused our attention only on compounds with inhibitory potency higher than 50% at that concentration. Furthermore, to test whether hits quench the AMC signal, inhibit the detection enzyme trypsin or are autofluorescent compounds, all promising candidates were subjected to counter-analysis in order to exclude false positives and false negatives (data not shown). Compounds showing no assay interference and a dose-dependent activity were then tested on hSirt2 to evaluate their selectivity.

Among the 592 tested compounds, we identified three hits characterized by potency in the low micromolar range: TCMDC-143159 (**5**), TCMDC-143362 (**6**) and TCMDC-143295 (**7**) (Figure 5). Due to reported toxicity of the anabasine ring,[60] present in **5**, we decided initially to resynthesize **6** and **7** to confirm their activity, and to modify their structures in order to obtain analogues with improved activity and selectivity profiles. Since the inhibition of hSirt2 is an undesired feature in new antischistosomials, but might identify new scaffolds for optimization of human sirtuin inhibitors we followed the lead of **6** as an unselective compound to some extent but focused mostly on the selective compound **7**.

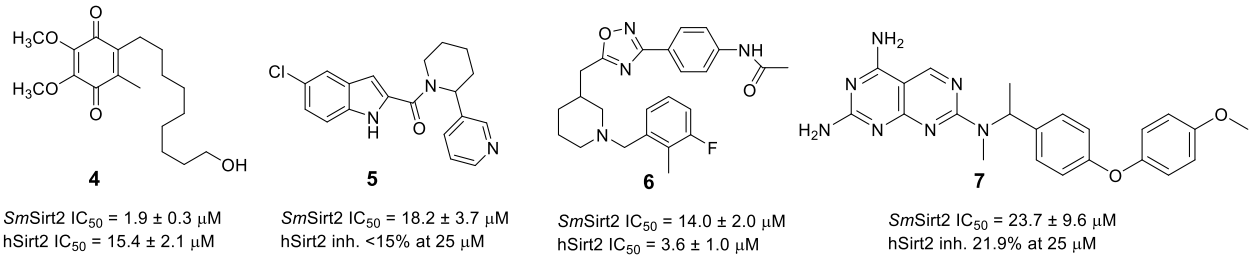

Figure 5. Structures and *in vitro* data of idebenone (**4**) and hits from the Kinetobox library (**5-7**). For IC_{50} values, errors are represented as ± SEM (n = 3).

Synthesis and initial SAR of 1,2,4-oxadiazolyl compound 6.

As previously cited, Feldmann *et al.* recently published the crystal structure of hSirt2 in complex with myristoylated peptides, showing the placement of the acyl chain in a hydrophobic pocket and the conservation of this localization during the entire catalytic reaction.[37,53] Since this could also be the case in *Sm*Sirt2, after establishing its synthesis, initial optimization of **6** was attempted with the replacement of the acetyl group with a longer fatty acyl group, such as an octanoyl (**11**) or a decanoyl (**12**) chain, in order to potentially address such a pocket. The synthesis of **6** and its analogues **11** and **12** is outlined in Scheme 2. A nucleophilic substitution between the

commercially available 2-(piperidin-3-yl) acetic acid ethyl ester and 3-fluoro-2-methylbenzyl bromide was performed in order to obtain the intermediate **8**. The reaction between the requisite acyl chlorides and 4-aminobenzonitrile yielded the 4-cyanoanilides **9b** and **9c** which, together with the commercially available 4-cyanoacetanilide **9a**, were treated with hydroxylamine hydrochloride to give the benzamidoximes **10a-c**. Subsequent condensation between **10a**,**b** and **8** afforded the required compounds **6** and **11**, and the reaction between **10c** and the acyl chloride of **8**, obtained by hydrolysis of the ethyl ester and subsequent chlorination, gave the final compound **12**.

When tested against *Sm*Sirt2 and hSirt2 at 25 µM, the hit **6** was confirmed to have inhibitory activity from the newly synthesized sample whereas the octanoyl and decanoyl analogues **11** and **12** were practically inactive against both parasite and human enzymes (**6**: *Sm*Sirt2 IC_{50} = 14.5 ± 0.6 µM; hSirt2 IC_{50} = 8.0 ± 1.1 µM; **11**: *Sm*Sirt2 inh. 30.5%; hSirt2 inh. <15%. **12**: *Sm*Sirt2 inh. <15%; Sirt2 inh. <15%).

Scheme 2. Synthesis of compounds 6, 11 and 12.[a]

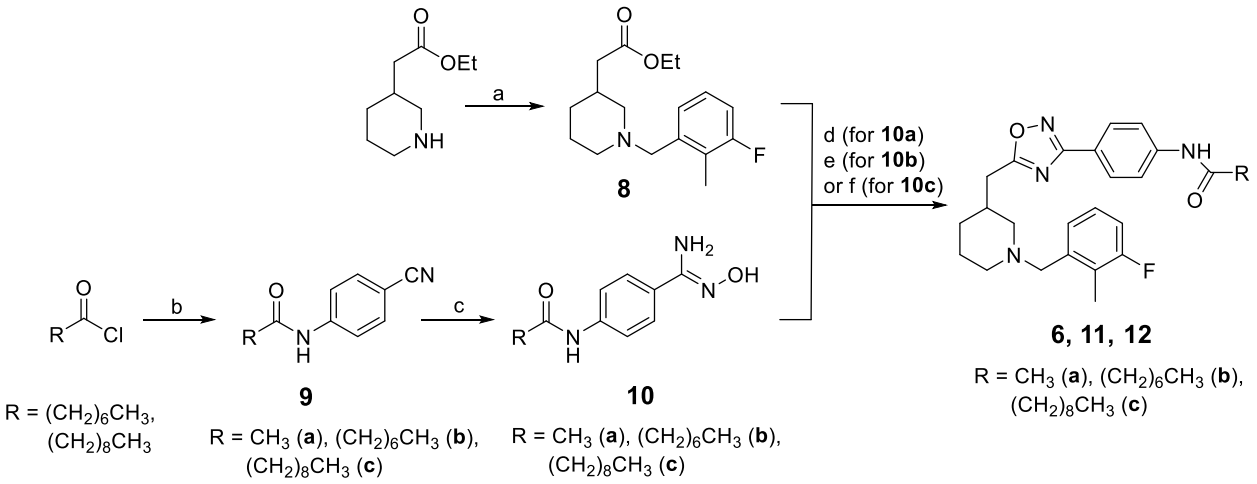

[a] Reagents and conditions: (a) 3-fluoro-2-methylbenzylbromide, triethylamine, toluene, 0 °C → rt, 18 h; (b) 4-aminobenzonitrile, triethylamine, dry DCM, 0 °C → rt, 2 h, N_2; (c) hydroxylamine hydrochloride, sodium carbonate, water/ethanol, reflux, 6-8 h; (d) **8**, **10a**, potassium carbonate, pyridine, reflux 8h, then rt 72 h; (e) **8**, **10b**, potassium carbonate, pyridine, microwave, 180 °C, 10 min, 300 Watt, then reflux 43 h and finally rt 12 h; (f) from **8**: i) 1M lithium hydroxide, ethanol, 20 h, rt; ii) thionyl chloride, DMF, dry DCM, -15 °C → r.t., 3h, N_2; iii) **10c**, triethylamine, DMF, dry DCM, rt, 22 h, then 150 °C 3 h, N_2.

Synthesis and SAR of pyrimidopyrimidine 7.

To work on the structure of the hit **7**, we started with a fragment-based approach with the development of analogues with a simplified structure, in order to identify the substructure(s) responsible of the inhibitory activity. In particular, since the 2,4,7-triaminopyrimidopyrimidine moiety of **7** ("part A", Figure 6) could mimic the adenosine part of NAD^+, we synthetized a first generation of analogues keeping this portion fixed and introducing several modifications at the Nα (Figure 6). More precisely, we purchased the parent pyrimido[4,5-*d*]pyrimidine-2,4,7-triamine **13** and prepared derivatives where the Nα is a secondary (**14**, **18** and **19**), tertiary (**20-**

23), or inserted in a cycle (**15-17**). While **14-17** are characterized by small amine substitution at the C7 position, the N^7-benzylpyrimido[4,5-*d*]pyrimidine-2,4,7-triamines **18-23** represent the most substituted compounds of the series, with changes at the Nα, Cβ and C4 benzyl positions ("part B", Figure 6).

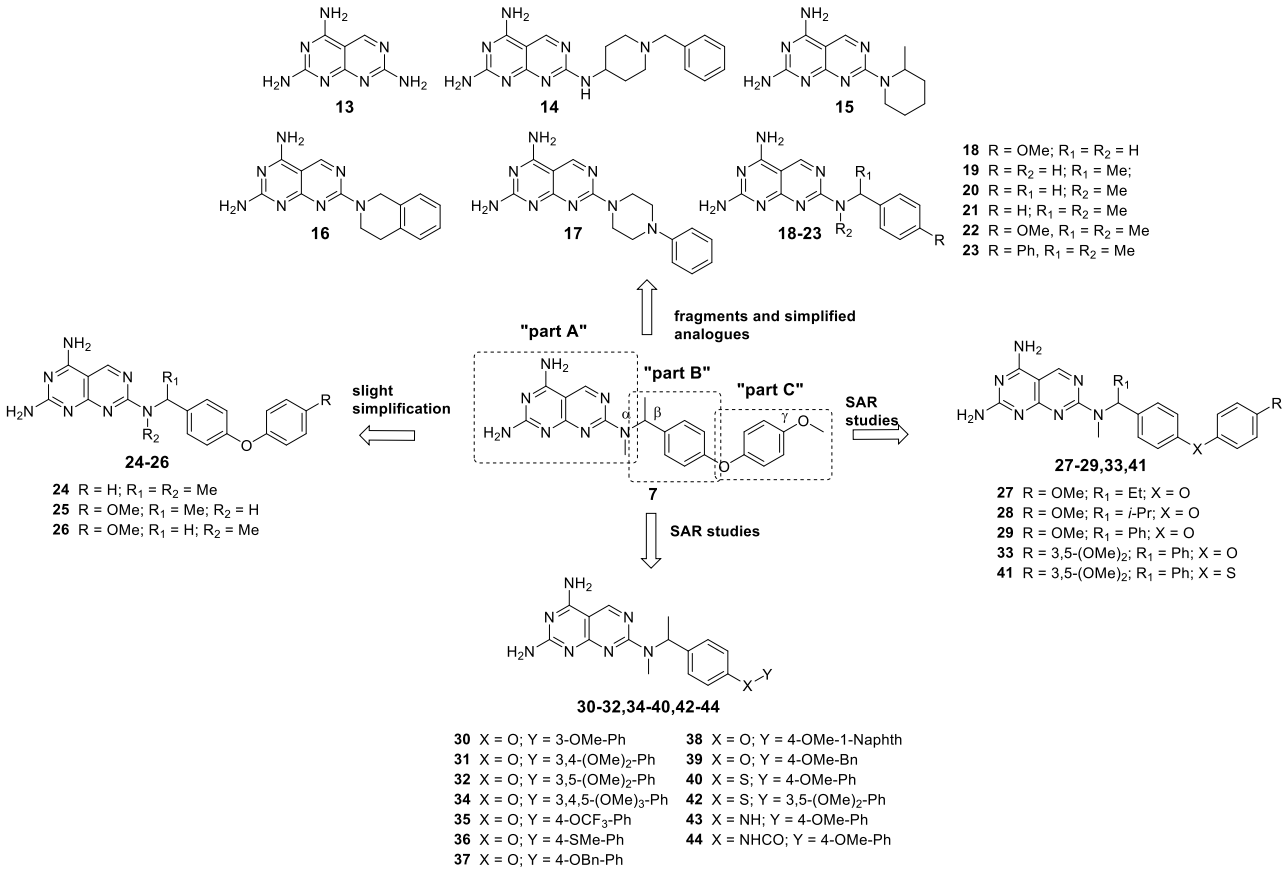

Figure 6. Overview of analogues of **7**: fragment-based approach and SAR studies.

As shown in Table 3 (see below), compounds **13-22** show complete loss of activity on *Sm*Sirt2 and remain inactive on the human enzyme. Among the simplified analogues, only **23** bearing a large phenyl substituent at the right part of the molecule (4-biphenyl portion, "part C", Figure 6) displayed low *Sm*Sirt2 inhibition. As a consequence, we designed a second generation of

analogues in which small focused modifications were applied, without leading to an excessive alteration of the prototype structure, but maintaining a high similarity to it. Specifically, we focused on the Nα, Cβ and Cγ positions of **7** (Figure 6) through the removal of the methyl or methoxy groups (**24-26**). We increased the steric hindrance of the Cβ substituent ("part B", Figure 6), by replacing the methyl with an ethyl, *iso*propyl, or phenyl group (**27-29**, **33**, **41**), and we explored the effect of replacement of the 4-methoxyphenoxy portion of **7** ("part C", Figure 6) with other substituted phenoxy, 1-naphthyloxy, benzyloxy, phenylthio, aniline and benzanilide moieties (**30-44**)**.**

Chemistry. The pyrimido[4,5-*d*]pyrimidine-2,4,7-triamine **13** is commercially available. The final compounds **14-44** were prepared by reaction between the commercial 4-amino-2-bromopirimidine-5-carbonitrile and the appropriate amines **46** in anhydrous 2-methoxyethanol, in the presence of triethylamine at 80 °C. The obtained pyrimidine intermediates **47** were converted into the desired compounds **14-44** through condensation reactions performed at 150 °C with the guanidine free base in dry 2-methoxyethanol (Scheme 3). The amines **46a-h** used for the synthesis of the pyrimidine intermediates **47a-h** are commercially available and were purchased from vendors. The amines **46i-f'**, useful synthons for the synthesis of the final compounds **22-44**, were prepared by reaction of the corresponding phenyl ketones or aldehydes **45a-w** with 7 M ammonia (for secondary amines) or 2 M methylamine (for tertiary amines) solution in anhydrous methanol in the presence of titanium *iso*propoxide at room temperature, followed by the addition, after the formation of the imine intermediates, of the reducing agent sodium borohydride at 0 °C under nitrogen atmosphere (Scheme 4A). The phenyl ketones/aldehydes **45a-e** are commercially available. The ketones **45f-q**,**s-u** were synthesized by reaction between the appropriate aromatic alcohols or thiols and the 1-(4-fluorophenyl)ethan-1-one, -propan-1-one, -2-methylpropan-1-one, and -(phenyl)methanone in the presence of anhydrous potassium carbonate in dry DMF at 175 °C

(Scheme 4B). The 1-(4-((4-methoxybenzyl)oxy)phenyl)ethan-1-one **45r**,[61] the 1-(4-((4-methoxyphenyl)amino)phenyl)ethan-1-one **45v**,[62] and the N-(4-acetylphenyl)-4-methoxy-benzamide **45w**[63] were prepared according to the literature. For the structures of the intermediates **45-47** see Supporting Information.

Scheme 3. Synthesis of compounds 7, 14-44.[a]

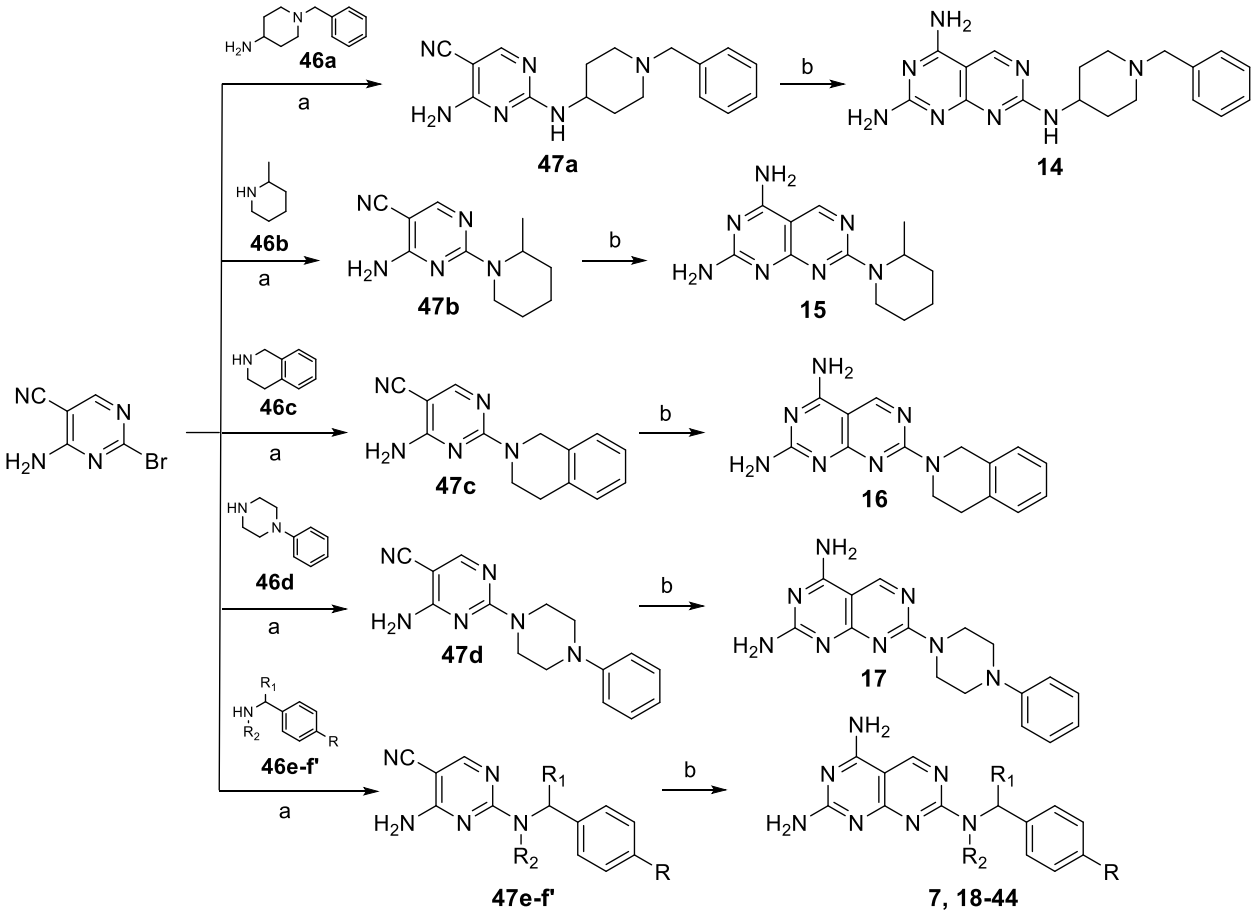

[a]Reagents and conditions: (a) triethylamine, dry 2-methoxyethanol, 80 °C, 2.5-8 h; (b) guanidine free base, dry 2-methoxyethanol, 150 °C, 1.5-4.5 h.

Scheme 4. Synthesis of the intermediate compounds 45 and 46.[a]

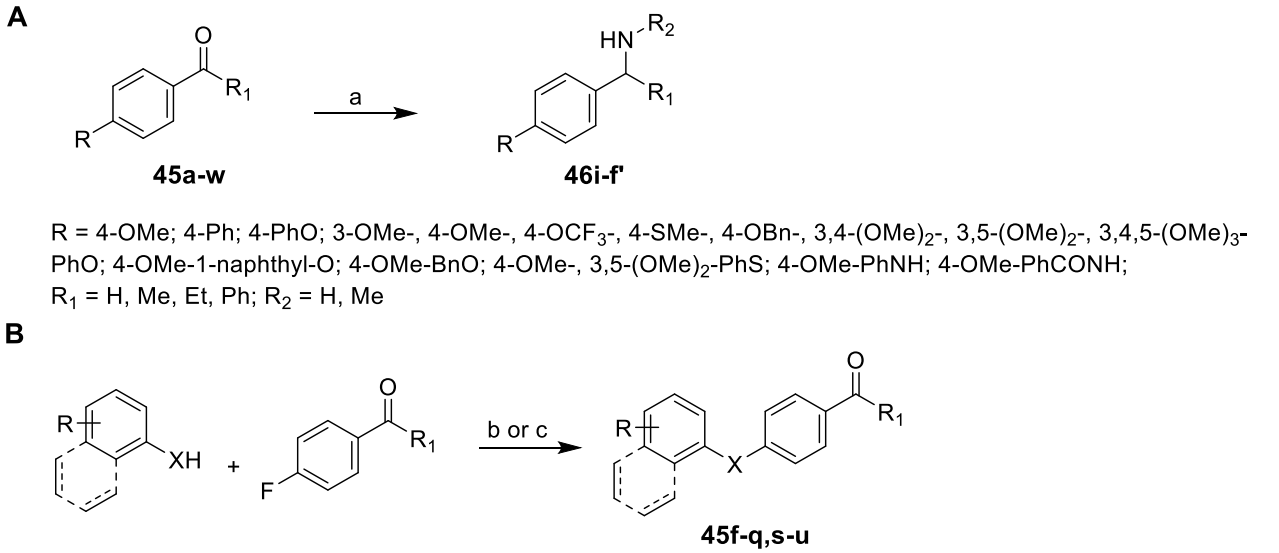

[a]Reagents and conditions: (a) anhydrous potassium carbonate, dry DMF, 175 °C, 5 h; (b) 2 M methylamine in methanol, titanium *iso*propoxide, dry THF, N_2, 5-6 h, rt, then sodium borohydride, N_2, 2 h, rt; (c) 7 M ammonia in methanol, titanium *iso*propoxide, N_2, 5 h, rt, then sodium borohydride, N_2, 2 h, rt.

All the above compounds were tested in vitro against *Sm*Sirt2[47] and hSirt2, to study their selectivity for the parasitic enzyme (Table 3).[59] An amine and a pyrimidine synthetic intermediates (**46k** and **47m**, see Table S5 for their structures) were also included in the list, to confirm the importance of the intact pyrimido[4,5-*d*]pyrimidine-2,4,7-triamine scaffold for the inhibiting activity. The percentages of inhibition at 25 μM or the IC_{50} values of the new compounds tested against *Sm*Sirt2 as well as hSirt2 are reported in Table 3.

Table 3. *In vitro* inhibition of *Sm*Sirt2 and hSirt2 by 7, 13-44, 46k, and 47m.

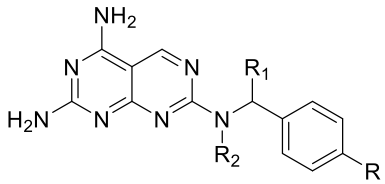

compd	R	R_1	R_2	*Sm*Sirt2[a] % inhibition at 25 μM or IC_{50} [μM]	hSirt2[a] % inhibition at 25 μM or IC_{50} [μM]
7	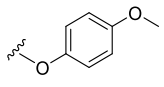	Me	Me	23.7 ± 9.6	21.9%
13[b]				<15%	<15%
14[b]				<15%	23.2%
15[b]				<15%	<15%
16[b]				<15%	<15%
17[b]				<15%	<15%
18	-OMe	H	H	<15%	<15%
19	H	Me	H	<15%	<15%
20	H	H	Me	<15%	<15%
21	H	Me	Me	<15%	<15%
22	-OMe	Me	Me	<15%	<15%
23	-Ph	Me	Me	24.8%	<15%
24	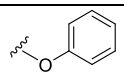	Me	Me	27.6%	<15%
25	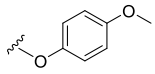	Me	H	37.5%	21.0%
26	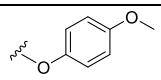	H	Me	<15%	<15%

27	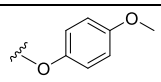	Et	Me	12.8 ± 0.8	36.7 ± 7.7
28	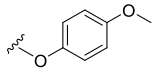	*i*-Pr	Me	27.7 ± 3.8	57.4%
29	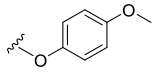	Ph	Me	2.34 ± 0.2[c]	22.1%
30	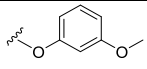	Me	Me	23.1 ± 1.4	33.8%
31	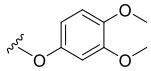	Me	Me	44.7 ± 4.4	35.3%
32	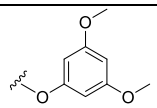	Me	Me	12.5 ± 1.1	7.4%
33	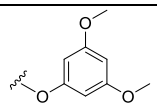	Ph	Me	3.3 ± 0.2	29.6%
34	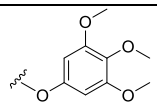	Me	Me	30.8 ± 3.0	29.2%
35	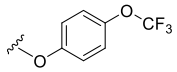	Me	Me	20.3%	37.5%
36	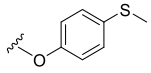	Me	Me	49%	<15%
37	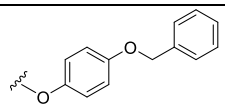	Me	Me	40.3%	70.4%
38	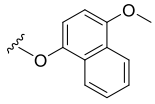	Me	Me	18.4%	30.6%
39	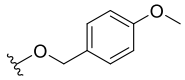	Me	Me	46.2%	61.7%
40	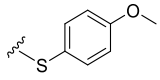	Me	Me	14.9 ± 0.9	13.3 ± 1.6

41	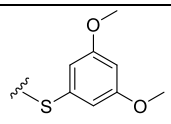	Me	Me	4.3 ± 0.4	27.9%
42	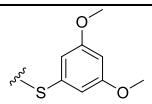	Ph	Me	2.0 ± 0.1	21.5 ± 3.1
43	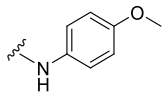	Me	Me	65.1 ± 7.2	40.8%
44	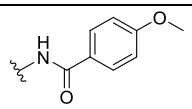	Me	Me	41.9%	<15%
46k[d]				<15%	<15%
47m[d]				<15%	<15%

[a]IC_{50} ± SEM are reported (n=3). [b]For chemical structures see Figure 6. [c]maximum of observed inhibition: 60%. [d]For chemical structures see Table S5 in Supporting Information.

As stated above, none of fragments or simplified molecules **13-22** showed inhibitory activity on either the parasite or human enzymes. Only the derivatives carrying the 1-([1,1'-biphenyl]-4-yl)ethyl (**23**) or 1-(4-phenoxyphenyl)ethyl (**24**) substituent at Nα (Figure 6) partially retained inhibition against *Sm*Sirt2, demonstrating the crucial role of the substituted phenoxyphenyl or 1,1'-biphenyl portion at the right side of the molecule ("part C", Figure 6). The removal of the methyl group at either the **7** Nα (see **25**) or Cβ position (see **26**) (Figure 6) decreased or totally abolished the *Sm*Sirt2 inhibitory activity, respectively. In contrast, the insertion at Cβ of groups bigger than methyl [ethyl (**27**), *iso*propyl (**28**), and phenyl (**29**)], generally improved the *Sm*Sirt2 inhibitory potency up to 10-fold, reaching with **29** the single-digit micromolar level (IC_{50} = 2.34 µM). Interestingly, **29** is more selective than **7** for *Sm*Sirt2 over hSirt2 as judged by IC_{50} values, but it reaches only a maximum of inhibition of 60 % which complicates the interpretation of the

selectivity data. The *iso*propyl derivative **28** was an exception, displaying similar inhibitory potency as **7** against *Sm*Sirt2, and higher potency against hSirt2.

At the "part C" of the molecule (4-methoxyphenoxy moiety, Figure 6), no particular increase in activity or selectivity was obtained with the shift of the methoxy group from *para* to *meta* position (**30**), and the introduction of 3,4-dimethoxy (**31**) or 3,4,5-trimethoxy (**34**) groups at the phenoxy portion, as well as the replacement of the 4-methoxy with a 4-trifluoromethoxy (**35**), 4-methylthio (**36**), or 4-benzyloxy (**37**) group reduced the inhibitory potency against *Sm*Sirt2. However, the insertion of two methoxy groups at 3,5 position of the phenoxy moiety (**32**) led to 2-fold increase of potency against *Sm*Sirt2 and improved selectivity over hSirt2. In this last compound, the further replacement of the methyl group at Cβ with a phenyl ring (**33**) determined an additional increase of potency against *Sm*Sirt2 (IC_{50} = 3.3 μM, 7-fold higher potency compared to **7**), confirming the positive SAR about Cβ substitution with large groups. The replacement of the 4-methoxyphenoxy moiety of **7** with the larger 4-methoxy-1-naphthyloxy (**38**) or the longer 4-methoxybenzyloxy (**39**) group led to a decrease in potency against *Sm*Sirt2 and, in the case of **39**, improved hSirt2 inhibition. Again in the 4-methoxyphenoxy group, the isosteric change oxygen-sulphur atom led to the 4-methoxyphenylthio analogue **40**, which produced a 1.6-fold enhancement of *Sm*Sirt2 inhibition (IC_{50} = 14.9 μM), combined with improved inhibition of the human enzyme (IC_{50} = 13.3 μM). The further change from the 4-methoxy to the 3,5-dimethoxy substitution at the phenylthio moiety of **40** provided **41**, that showed improved potency and selectivity against *Sm*Sirt2 (*Sm*Sirt2 IC_{50} = 4.3 μM, hSirt2 inhibition = 27.9 % at 25 μM). Moreover, the combination of the positive SAR of the series with the replacement of the Cβ methyl of **41** with the Cβ phenyl group gave **42**, the most potent compound of the series vs *Sm*Sirt2 (IC_{50} = 2 μM) and 10-fold selective over the human counterpart hSirt2 (IC_{50} = 21.5 μM).

The replacement of the 4-methoxyphenoxy portion with a 4-methoxyaniline (**43**) or 4-methoxybenzamide (**44**) group led to a decrease in potency against *Sm*Sirt2. Finally, the total absence of inhibitory activity against both parasitic and human enzymes by the intermediates **46k** and **47m** confirmed the importance of the intact pyrimido[4,5-*d*]pyrimidine-2,4,7-triamine scaffold ("part A", Figure 6) for the inhibitory activity of such compounds. The inhibing activity of selected compounds **33**, **36**, **41**, **42** and **44** was also evaluated in the presence of the myristoylated substrate **3f** instead of the acetylated **1**. As reported in Table 4, in many cases no significant inhibition was measured in the presence of *Sm*Sirt2 and hSirt2 with the exception of **33**, **41** and **42**, which show an inhibitory potency for the hSirt2 catalyzed demyristoylation in the low micromolar range. This may present a new starting point for the development of human Sirtuin inhibitors with a selectivity for long chain acyl removal, as so far a preference, if any, has been observed only for deacetylation.

Table 4. Inhibitory activity of selected compounds 33, 36, 41, 42, and 44 against *Sm*Sirt2 and hSirt2 with myristoylated 3f as substrate.

Compound	***Sm*Sirt2 (3f)** **IC_{50} [µM][a] or % inhibition at 20 µM**	**hSirt2 (3f)** **IC_{50} [µM][a] or % inhibition at 20 µM**
7	16.8 ± 1.14[b]	<15%
33	<15%	13.1 ± 2.2
36	<15%	38.1%
41	15%	25.1 ± 4.1
42	<15%	15.6 ± 1.9
44	<15%	<15%

[a]IC_{50} values are reported as ± SEM (n=3). [b]maximum of inhibition: 45 %.

***In vitro* effects on schistosomula and adult worms.**

In order to evaluate whether these optimized compounds have effects on the parasite, **29**, **32**, **33** and **41** together with the prototype **7** were tested on schistosomula and adult worms. Two potential negative controls **26** and **39** were also included in the series. As shown in Figure S1, all tested compounds reduce the viability of cultured schistosomula at 10 and 20 µM, including **26** and **39**, which show low or no activity on the recombinant enzyme (Table 3).

Experiments on adult worms report a similar trend (Figure 7), where again the *Sm*Sirt2 inhibitors as well as the potential negative controls reduce worm pairing and egg laying already after 24 hours of culture. Whilst the possibility that the enzyme inhibitors do exert their effects via inhibition of *Sm*Sirt2 cannot be ruled out, the strong effects that **26** and **39** also have on parasite viability and reproduction indicate that the effects of compounds shown in Figure 7 on the parasite may be at least in part due to the modulation of other targets (off-target effects).

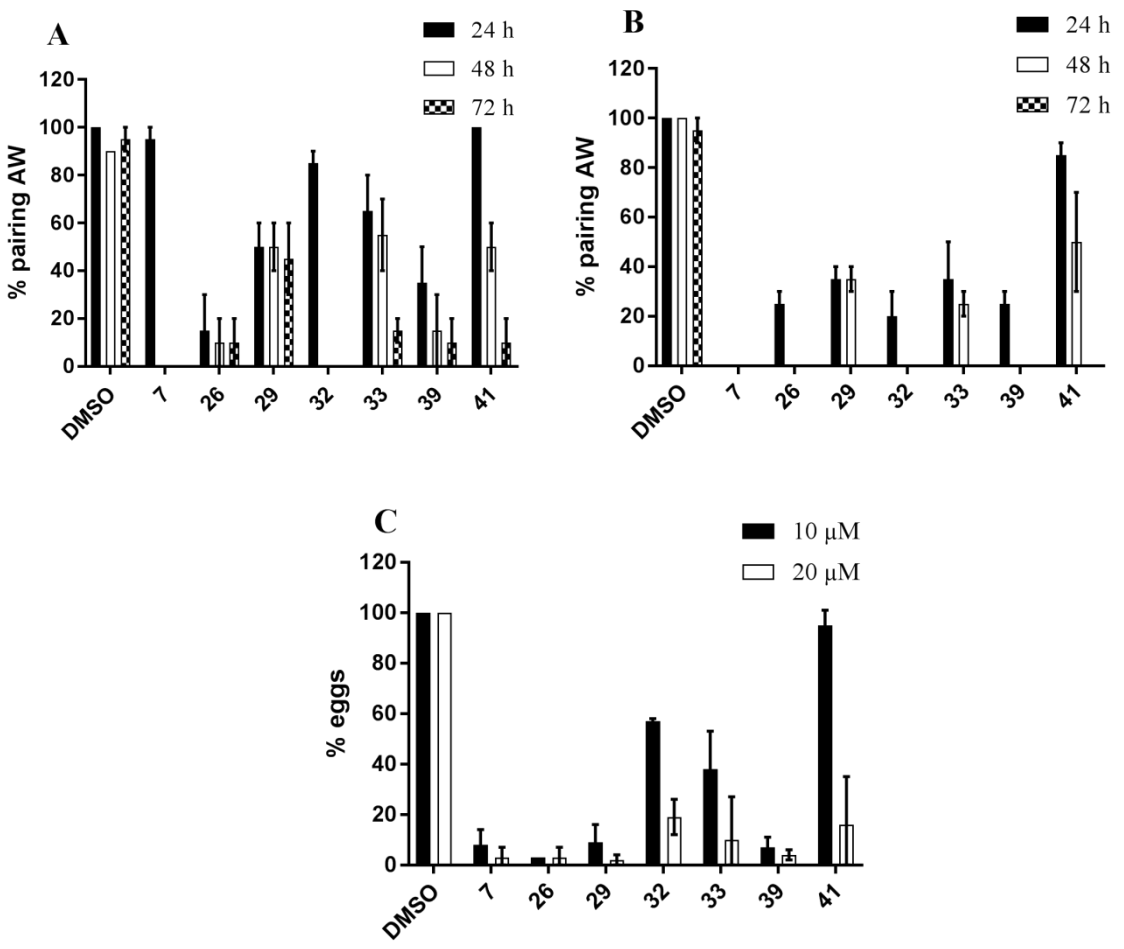

Figure 7. Effects of **7** and its analogues on adult worms (AW) pairing at 10 µM and 20 µM (**A** and **B** respectively). Assay used: microscopy examination. Results after 24, 48 and 72 hours are represented with black, white and chequered bars respectively. Effect of these compounds on egg laying (**C**). Compounds **26** and **39** do not block *Sm*Sirt2 in-vitro.

To get some further insight, we measured selected compounds **7**, **26**, **29**, **32**, **33**, **39** and **41** for toxicity on human cultured cancer cells using a MTS viability assay. In this assay, the compounds that are inactive on *Sm*Sirt2 but active on schistosomes also show toxicity on the human cells while the *Sm*Sirt2 inhibitors with activity on the worms do not show this general toxicity (see Figure 8).

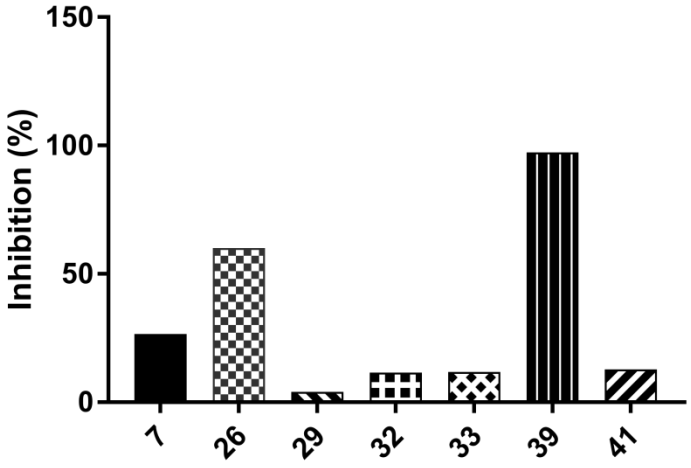

Figure 8. Growth inhibition of HL-60 acute myeloid leukaemia cells by compound **7** and selected analogues at 10 μM assay concentration.

Conclusion. The identification of a robust deacylase activity of *Sm*Sirt2, supported by kinetic investigations, expands the range of possible biological activities relevant for *Sm*Sirt2. The high demyristoylation efficiency of this enzyme suggests the merit of undertaking future investigations on deacylation inhibition, rather than deacetylation inhibition, as a new strategy to kill both schistosomula and adult worms. For inhibitors of hSirt2 with a thiomyristoylated lysine core (also called TM), it has been proposed that a dual deacetylase/demyristoylase activity is beneficial for cellular potency in cancer cells and selectivity over non-cancer cells.[64]

With the aim of finding potent and selective inhibitors of *Sm*Sirt2, we performed screening of the GSK-kinetobox library, composed of 592 compounds with proven activity against cultured kinetoplastids, namely *Leishmania donovani*, *Trypanosoma cruzi* and *Trypanosoma brucei*. From an initial test we identified **5**, **6** and **7** as valuable hits for further optimization. As outlined above, we focused our attention on **6** and **7**. Regarding **6**, the attempt to potentially target the enzymatic (possibly extended) C pocket through an octanoylated and decanoylated analogue, led to a loss in activity. Extensive SAR studies performed on **7** highlighted the crucial role of the presence of the intact pyrimido[4,5-*d*]pyrimidine-2,4,7-triamine ("part A" of the molecules), disubstituted at N7 (Nα in Figure 6) with a methyl and a substituted 1-phenylethyl moiety ("part B"), further carrying a substituted phenoxy/phenylthio group at its C4 position ("part C"), recognized as crucial to elicit *Sm*Sirt2 inhibitory potency and selectivity over hSirt2 (Figure 6). In particular, the presence at "part C" of the 4-methoxyphenoxy, 3,5-dimethoxyphenoxy and 3,5-dimethoxyphenylthio portion, combined with the the phenyl group at Cβ position ("part B") led to the most potent derivatives **29**, **33**, **41**, and **42** with IC_{50} values in the single-digit micromolar range for *Sm*Sirt2. Experiments with **7** and its analogues on schistosomula and adult worms showed strong activity but also from enzymatically inactive compounds. However, while the inactive *Sm*Sirt2 inhibitors

26 and **39** also showed unspecific toxicity to human cancer cells, the selective *Sm*Sirt2 inhibitors **7**, **29**, **32**, **33** and **41** were non-toxic to human cancer cells.

Thus, for the first time, we can show that *Sm*Sirt2 can be drugged with selectivity over the human isotype (especially **29**, **33** and **41**) and the inhibitors block *Schistosoma* growth without general toxicity to human cells. This can be used as starting point for further optimization studies. In addition, leads for new inhibitors of hSirt2 have been identified, interestingly some with a preference for demyristoylation over deacetylation.

ACKNOWLEDGMENTS

This work was supported by Deutsche Forschungsgemeinschaft (DFG, GRK1976, to D.M. and M.J., testing on human Sirtuins Ju295/14-1), Italian PRIN 2015 (prot. 20152TE5PK to A.M.), AIRC 2016 (n. 19162 to A.M.), Progetto Ateneo Sapienza 2017 (to D.R.), the A-ParaDDisE program funded under the European Union's Seventh Framework Programme (grant agreement no. 602080 to M.J., C.R., R.P., A.M.) This study was supported by the grant ANR-10-LABX-0030-INRT, a French State fund managed by the Agence Nationale de la Recherche under the frame program Investissements d'Avenir ANR-10-IDEX-0002-02 to C.R., M.M. and E.R-M. J.L. and R.J.P. are supported by institutional funds from the Centre National de la Recherche Scientifique (CNRS), the Institut National de la Sante et de la Recherche, Medicale (INSERM), the Institut Pasteur de Lille and the Universite de Lille. We thank GSK for kindly donating the Kineto Boxes compounds (aka TCKAS) for biological testing and the COST action CM1406 (Epigenetic Chemical Biology) for support.

ABBREVIATIONS USED

AMC, 7-amino-4-methylcoumarin; NA, nicotinamide; Z-Lys-OH, benzyloxycarbonyl lysine.

EXPERIMENTAL SECTION

Recombinant production and purification of *Sm*Sirt2. Recombinant expression and purification of *Sm*Sirt2 was done as previously described.[47] Briefly, overexpression was carried out in *E. coli* BL21(DE3) cells in 2 x Luria Broth (2 x LB) medium. The cells were grown to $O.D._{600}$ of 1.2 at 37°C, then the culture was cooled down to 25°C and induction of expression was done by adding 0.5 mM final isopropyl-1-thio-β-D-galactopyranoside (IPTG, Euromedex), in presence of 100 µM $ZnCl_2$. Harvested bacteria were resuspended in lysis buffer (400 mM NaCl, 10 mM Tris-HCl pH 8.0) and lysed by sonication. The lysate was clarified by centrifugation (17,000 rpm, JA-25.50 Beckman) for 1 h. The supernatant was loaded onto Talon Metal affinity resin (Clontech) pre-equilibrated with the lysis buffer. The 3C protease treatment was used to remove His-tag from the recombinant protein, which was subsequently loaded onto HiLoad 16/60 Superdex 200 gel filtration column (Amersham Bioscience) equilibrated in 400 mM NaCl, 10 mM Tris-HCl pH 8.0, and 2 mM DTT. Finally, the protein was concentrated with an Amicon Ultra centrifugal filter units (Millipore) to reach a final concentration of 1.5 mg/ml as assayed by the A280 measurement (NanoDrop).

Long chain deacylation. Theoretical conversion of **3a-g** by *Sm*Sirt2 and hSirt2 and their inhibition were evaluated by homogeneous assay using 10.5 µM assay concentration of potential substrates (prepared from 12.6 mM stock solution in DMSO and diluted with assay buffer) instead of **ZMAL**. Regarding hSirt2, 25 mM HEPES, 137 mM NaCl, 2.7 mM KCl, 1 mM $MgCl_2$, 0.015% Triton X-100, pH= 8.0 was used as assay buffer. OriginPro 9.0 G and GraphPad 7.0 were used for the analysis of results.

Kinetic analysis of PSDKac and PSDKmyr. Deacylation reactions were evaluated by reversed phase HPLC (Kinetex XB-C18 column, 100 Å, 5 µm, 250 x 4.6 mm) by monitoring the formation of the deacylated product at 214 nm. Linear deacylation rates were determined by

incubation of 47 µL of *Sm*Sirt2 solution (104 ng/µL, final assay concentration 80 ng/µL) in assay buffer (25 mM HEPES, 137 mMNaCl, 2.7 mMKCl, 1 mM $MgCl_2$, 0.015% Triton X-100, pH = 8.0) with 3 µL of DMSO, 5 µL of PSDKac (Ac-Pro-Ser-Asp-Lys(acetyl)-Tyr-Ile-Gly-Gly-Trp-Trp-NH_2custom synthesized by PSL, Heidelberg, Germany) or PSDKmyr (Ac-Pro-Ser-Asp-Lys(myristoyl)-Tyr-Ile-Gly-Gly-Trp-Trp-NH_2 custom synthesized by PSL, Heidelberg, Germany) solution (prepared from 3.6 mM stocks in DMSO and diluted with assay buffer, concentration ranges 10-300 µM) and 5 µL of NAD^+ (prepared from 6 mM stock in assay buffer and diluted in assay buffer, final assay concentration 500 µM). At 0, 1, 3, 5, 10, 20 and 30 minutes the deacylation was quenched with 6.7 µL of TFA (10% in assay buffer, final assay concentration 1%), incubated for 5 min at 37 °C and then centrifuged for 10 minutes at 14000*g*. 55 µL of the supernatant were transferred into HPLC vials and analysed. Each experiment was done twice in duplicate. HPLC method to evaluate the deacylation: eluent A, H_20 + 0.05% TFA; eluent B, acetonitrile + 0.05% TFA; 0 - 4 min, linear increase from B = 10% to B = 40%; 4 - 10 min, linear increase to B = 60%; 10 min, linear increase to B = 100%; 10-14 min, B = 100%; 14-16 min, linear decrease to B = 10%; 16 – 25 min, B = 10%) with a flowrate of 1 mL/min. The following method has been used to follow demyristoylation reactions: eluent A, H_20 + 0.05% TFA; eluent B, acetonitrile + 0.05% TFA; 0 - 5 min, linear increase from B = 10% to B = 40%; 5–8.5 min, linear increase to B = 80%; 8.5-9.5 min, linear increase to B = 90%; 9.5-10.5 min, linear increase to B = 100%; 10.5-15 min, B = 100%; 15 min, B = 100%; 15 – 18 min, linear decrease to B= 10%) with a flowrate of 1 mL/min. The quantification of product peaks allowed the determination of deacylation rates and the data have been fitted to the Michaelis-Menten equation. GraphPhad Prism has been used to determine K_m, k_{cat}, k_{cat}/K_m.

Kinetic analysisof NAD^+_{PSDKac} and $NAD^+_{PSDKmyr}$. Deacylation reactions were evaluated by reversed phase HPLC (Kinetex XB-C18 column, 100 Å, 5 µm, 250 x 4.6 mm) by monitoring the formation of the deacylated product at 214 nm. Linear deacylation rates have been determined by incubation of 47 µL of *Sm*Sirt2 solution (104 ng/µL, final assay concentration 80 ng/µL) in assay buffer (25 mM HEPES, 137 mM NaCl, 2.7 mM KCl, 1 mM $MgCl_2$, 0.015% Triton X-100, pH= 8.0) with 3 µL of DMSO, 5 µL of PSDKac or PSDKmyr (prepared respectively from 2.4 mM and 0.96 mM stock in DMSO and diluted with assay buffer, saturating assay concentrations) and 5 µL of NAD^+ (prepared from 6 mM stock in assay buffer and diluted with assay buffer. NAD^+ assay concentration range 10-250 µM). At 0, 1, 3, 5, 10, 20 and 30 minutes the deacylation was quenched with 6.7 µL of TFA(10% in assay buffer, final assay concentration 1%), incubated for 5 min at 37 ^{0}C and then centrifuged for 10 minutes at 14000*g*. 55 µL of the supernatant have been transferred into HPLC vials and analysed. Each experiment was done twice in duplicate. Deacetylation and demyristoylation were evaluated using the same HPLC methods described for PSDKac and PSDKmyr respectively. The quantification of product peaks allowed the determination of deacylation rates, and the data have been fitted to the Michaelis-Menten equation. K_{m,NAD^+}, k_{cat,NAD^+} and k_{cat}/K_m have been determined by the use of GraphPhad Prism 7.0.

***In vitro* Kinetobox screening (*Sm*Sirt2).** For the screening of the Kinetobox library a homogeneous fluorescence based assay, developed in our group, was used to determine *Sm*Sirt2[56] activity. OriginPro 9.0 G was employed to determine IC_{50} values. Absence of eventual assay interference due to trypsin inhibition was confirmed according published procedures[56] (data not shown), while, to exclude any quenching of the AMC signal, 2.5µL of a AMC solution (prepared from 12.6 mM stock solution in DMSO and diluted with assay buffer, final assay concentration, 10.5 µM) were used instead of ZMAL in the homogeneous assay. Active compounds were tested for known classes of assay interference compounds with the publicily available online tool “False

Positve Remover" (www.cbligand.org). The only compound flagged as PAINS was the approved drug Idebenone but none of our leads or analogues in the optimization campaign.

***In vitro* inhibition of hSirt2.** The activity of potential hits on hSirt2 was measured according published procedures.[59] All compounds were initially tested at 25 μM and, for candidates that showed a hSirt2 inhibition equal or higher than 50% at this concentration, IC_{50} values have been measured and determined using OriginPro 9.0 G.

General chemistry conditions. Reagents, starting materials and solvents were used without further purification of the purchased form. All reactions were monitored by Thin-layer chromatography (TLC) with Merck precoated silica gel 60 F_{254} plates and analysed under UV light (254 nm) using different mobile phases. Microwave assisted reactions were performed using a Discover S-1863 microwave system (CEM GmbH, Germany) and Biotage Initiator (Uppsala, Sweden) high frequency microwave synthesizer working at 2.45 GHz, fitted with magnetic stirrer and sample processor; reaction vessels were Biotage microwave glass vials sealed with applicable cap; temperature was controlled through the internal IR sensor of the microwave apparatus. Synthesized compounds were purified by flash column chromatography with a Biotage Isolera One automated flash purification system with UV-vis detector. TELOS Flash-LL silica columns 60 M were used as stationary phase with a mobile phase as specified in the following description. Yields were not optimized. Proton (^{1}H), carbon (^{13}C) and fluorine (^{19}F) spectra were recorded on Bruker Avance III HD spectrometer at 400, 100 and 376 MHz respectively, in reference to the solvents reported in the description. Chemical shifts δ are given in parts per million (ppm) and the peak assignment was supported by COSY and HSQC experiments. The purity of compounds **2**, **3**, **6**, **8-12** was determined by HPLC (UV detection at λ= 210 nm) and was equal to or higher than 95 % using the following conditions: eluent A, H_2O + 0.05% TFA; eluent B, acetonitrile + 0.05% TFA; linear gradient conditions (0-29 min, linear

increase from A = 100% and B = 0% to A = 0% and B =100%; 29-31 min, B = 100%; 31 min, decrease to B = 10%; 31-40 min B = 10%) with a flow rate of 1 mL/min; analytical column: Phenomenex Synergi 4 µm HYDRO-RP 80 Å, 250 mm X 4.6 mm for **3e**, **3f**, **3b**, **3c**, **3g** and **11**; Phenomenex Kinetex 5 µm XB-C18 100 Å, 250 mm X 4.6 mm for **3a**, **3d**, **6** and **12**. Low resolution mass spectra of compounds **7**, **14-44** were recorded on an API-TOF Mariner by Perspective Biosystem (Stratford, Texas, USA), samples were injected by a Harvard pump using a flow rate of 5-10 µL/min, infused in the Electrospray system. High resolution mass spectrometry (HR-MS) with electrospray ionization (ESI) analysis was performed using an Thermo Scientific Exactive mass spectrometer and for low resolution mass spectrometry with electrospray ionization (ESI) analysis was performed using Advion expression CMS spectrometer, with electron ionization (EI) on an Agilent Tecnologies 6890 N Network GC-MS system. Elemental analysis has been used to determine the purity of compounds **7**, **14-44** that resulted always >95%. Analytical results are within ± 0.40% of the theoretical values. All chemicals were purchased from Sigma Aldrich srl, Milan (Italy) or from TCI Europe NV, Zwijndrecht (Belgium), and were of the highest purity. As a rule, samples prepared for physical and biological studies were dried in high vacuum over phosphorus pentoxide for 20 h at temperatures ranging from 25 to 40 °C, depending on the sample melting point. General procedures and spectral data for the syntheses of the final compounds **7**, **14-44** are described below, while their chemical and physical data are reported in Table S4 in Supporting Information. Chemical, physical and ^{1}H-NMR spectral data for all unknown compounds among intermediates **45-47** are reported in Table S5. Elemental analysis for final compounds **7, 14-44** is reported in Table S6 in Supporting Information.

General procedure for the synthesis of 2-Benzyloxycarbonylamino-6-acylamino-hexanoic acid compounds (2a-d and 2g). To an ice-cold solution of Z-lysine (1 equiv, 5.35-6.24 mmol,

1.50-1.75 g) in 5.35-6.24 mL of 1M NaOH (1 equiv, 5.35-6.24 mmol) and water (8 equiv, 42.80-49.92 mmol, 42.80-49.92 mL), 1 equiv of acylchloride (5.35-6.24 mmol, 0.57-1.19 g, 0.55-1.29 mL) in dry THF (1 equiv, 5.35-6.24 mmol, 5.35-6.24 mL) and 5.35-6.24 mL 1M NaOH (1equiv, 5.35-6.24 mmol) were added drop by drop. After 20-45 minutes, the reaction was saturated with $NaCl_{ss}$, cooled below 0 °C and acidified to pH = 1.0 with 2M HCl. The product was extracted with ethyl acetate (four times, 60 mL each) and the combined organic layers extracted with 5% Na_2CO_3 (four times, 60 mL each). The bicarbonate solution was acidified with 2M HCl to pH = 1.0 and extracted with ethyl acetate (four times, 60 mL each). The combined organic extracts were washed with $NaCl_{ss}$, dried over Na_2SO_4 followed by evaporation of the solvent.

2-Benzyloxycarbonylamino-6-butyrylamino-hexanoic acid (2a). The crude product was purified by flash column chromatography on SiO_2 gel with DCM-methanol (96%-4%). Colorless oil; yield 5% (0.09mmol, 31.7 mg); rf = 0.09 (DCM-methanol 96%-4%). ^{1}H NMR (400 MHz, $CDCl_3$): δ = 7.34 (s, 5H, C*H* aromatic ring), 5.82 (s, 1H, N*H* amide), 5.72 (s, 1H, N*H* amide), 5.10 (s, 2H, CH_2 benzyl), 4.38–4.33 (m, 1H, C*H*NH), 3.33–3.17 (m, 2H, CH_2NH), 2.15 (t, ^3J(H,H) = 7.5 Hz, 2H, COCH_2), 1.91–1.73 (m, 2H,CH_2CH), 1.61 (m, 2H, CH_2CH$_3$), 1.56–1.47 (m, 2H, CH_2CH$_2$), 1.39 (m, 2H, CH_2CH$_2$), 0.91 ppm (t, ^3J(H,H) = 7.4 Hz, 3H, CH$_2$CH_3). MS (ESI), *m/z*: 349.0 $[M - H]^-$.

2-Benzyloxycarbonylamino-6-hexanoylamino-hexanoic acid (2b). The crude product was directly used for the next step without NMR.

2-Benzyloxycarbonylamino-6-octanoylamino-hexanoic acid (2c). Yield 95% (5.93 mmol, 2.41 g) of crude viscous oil; rf = 0.18 (DCM – methanol 96%-4%). ^{1}H NMR (400 MHz, $CDCl_3$): δ = 7.37–7.28 (m, 5H, C*H* aromatic ring), 6.04 (s, 1H, N*H* amide), 5.67 (d, ^3J(H,H) = 8.0 Hz, 1H, N*H* amide), 5.10 (s, 2H, CH_2 benzyl), 4.40-4.33 (m, 1H, C*H*NH), 3.29–3.18 (m, 2H, CH_2NH), 1.94–1.70 (m, 2H, CH_2CH), 1.65-1.58 (m, 2H, COCH_2), 1.55–1.48 (m, 2H, CH_2CH$_2$), 1.44–1.35

(m, 2H, C*H*$_2$CH$_2$), 1.30–1.24 (m, 10H, C*H*$_2$CH$_2$ octanoyl chain), 0.86 ppm (t, ^3J(H,H) = 6.4 Hz, 3H, CH$_2$C*H*$_3$). MS (ESI), *m/z*: 405.1 [M - H]$^-$.

2-Benzyloxycarbonylamino-6-decanoylamino-hexanoic acid (2d). The crude product was purified by flash column chromatography on SiO_2 gel with DCM-methanol (methanol gradient from1% to 10%). Colorless oil; yield 39% (2.31 mmol, 1.05 g); rf = 0.60 (DCM-methanol 95%-5%). ^{1}H NMR (400 MHz, $CDCl_3$): δ = 7.38–7.29 (m, 5H, C*H* aromatic ring), 5.85 (s, 1H, N*H* amide), 5.66 (s, 1H, N*H* amide), 5.10 (s, 2H, C*H*$_2$ benzyl), 4.40-4.36 (m, 1H, C*H*NH), 3.38–3.10 (m, 2H, C*H*$_2$NH), 2.18 (t, ^3J(H,H) = 7.6 Hz, 2H, COC*H*$_2$), 1.62–1.52 (m, 2H, C*H*$_2$CH), 1.63-1.58 (m, 2H, C*H*$_2$CH$_2$), 1.54–1.50 (m, 2H, C*H*$_2$CH$_2$), 1.47–1.35 (m, 2H, C*H*$_2$CH$_2$), 1.32–1.19 (m, 12H, C*H*$_2$CH$_2$ decanoyl chain), 0.87 ppm (t, ^3J(H,H) = 6.9 Hz, 3H, CH$_2$C*H*$_3$). MS (ESI), *m/z*: 433.3 [M - H]$^-$.

2-Benzyloxycarbonylamino-6-palmitoylamino-hexanoic acid (2g). Yield 73% **(**4.59 mmol, 2.38 g) of crude product as colorless oil; rf = 0.13 (DCM-acetonitrile 60%-40%). ^{1}H NMR (400 MHz, $CDCl_3$): δ = 7.35–7.28 (m, 5H, C*H* aromatic ring), 5.94 (s, 1H, N*H* amide), 5.10 (s, 1H, N*H* amide), 4,54 (s, 2H, C*H*$_2$ benzyl), 4.41–4.33 (m, 1H, C*H*NH), 3.29–3.17 (m, 2H, C*H*$_2$NH), 1.92–1.70 (m, 2H, C*H*$_2$CH), 1.62–1.55 (m, 2H, COC*H*$_2$), 1.54–1.47 (m, 2H, C*H*$_2$CH$_2$), 1.44-1.35 (m, 2H, C*H*$_2$CH$_2$), 1.31–1.25 (m, 26H, C*H*$_2$CH$_2$ palmitoyl chain), 0.88 ppm (t, ^3J(H,H) = 6.9 Hz, 3H, CH$_2$C*H*$_3$). MS (ESI), *m/z*: 517.5 [M - H]$^-$.

General procedure for the synthesis of 2-Benzyloxycarbonylamino-6-acylamino-hexanoic acid compounds (2e and 2f). 1 equiv. of myristc acid (3.50 mmol, 800 mg) or lauric acid (7.49 mmol, 1.5 g) were dissolved in 1 mL of dry DCM. Then 10 equiv of $SOCl_2$ (35.0-74.9 mmol, 4.16-8.91 g, 2.54-5.43 mL) were added. After 3 hours at 90 °C, the reaction was cooled to r.t. and $SOCl_2$ was removed by evaporation. The crude product was then dissolved in 4 mL of DCM dry and 1 equiv of Z-Lysine (3.50-7.49 mmol, 0.981-2.01 g) was added at 0 °C with 2 equiv of 2M

NaOH (7.0-14.98 mmol, 280-599 mg, 0.26-0.55mL). The reaction was left stirring for 20-72 h at rt. The reaction was then quenched by adding of 2N HCl to a pH of 2.0 and extracted three times with 20 mL of DCM. The combined organic phase was washed with $NaCl_{ss}$ and filtered over Na_2SO_4.

2-Benzyloxycarbonylamino-6-lauroylamino-hexanoic acid (2e). The crude product was purified by flash chromatography on SiO_2 gel with DCM-acetonitrile (acetonitrile gradient from 1% to 40%). Yellow oil; yield 12.7% (0.95 mmol, 439 mg); rf = 0.21 (DCM-acetonitrile 55%-45%). ^{1}H NMR (400 MHz, $CDCl_3$): δ = 7.37–7.26 (m, 5H, C*H* aromatic ring), 5.81 (s, 1H, N*H* amide), 5.73 (d, ^3J(H,H) = 7.8 Hz, 1H, N*H* amide), 5.09 (s, 2H, CH_2 benzyl), 4.45–4.33 (m, 1H, C*H*NH), 3.30–3.12 (m, 2H, CH_2NH), 2.19–2.10 (m, 2H, COCH_2), 1.93–1.71 (m, 2H, CH_2CH), 1.63–1.55 (m, 2H, CH_2CH$_2$), 1.53–1.46 (m, 2H, CH_2CH $_2$), 1.45–1.36 (m, 2H, CH_2CH$_2$), 1.31–1.24 (m, 16H, CH_2CH$_2$ lauroyl chain), 0.88 ppm (t, ^3J(H,H) = 6.9 Hz, 3H, CH$_2$CH_3). ESI-MS (-): 461.2 $[M - H]^-$.

2-Benzyloxycarbonylamino-6-myristoylamino-hexanoic acid (2f). A mixture of DCM-acetonitrile (acetonitrile gradient from 1% to 80%) was used to purify the crude product by flash chromatography on SiO_2gel. Colorless oil; yield 13.4% (0.470 mmol, 231 mg); rf = 0.35 (ethyl acetate–methanol 80%-20%). ^{1}H NMR (400 MHz, $CDCl_3$): δ = 7.37–7.31 (m, 5H, C*H* aromatic ring), 5.91 (s, 1H, N*H* amide), 5.70 (d, ^3J(H,H) = 7.8 Hz, 1H, N*H* amide), 5.14 (s, 2H, CH_2 benzyl), 4.42-4.36 (m, 1H, C*H*NH), 3.34–3.14 (m, 2H, CH_2NH), 2.20 (t, 2H, ^3J(H,H) = 7.2 Hz, COCH_2), 1.96–1.73 (m, 2H, CH_2CH$_2$), 1.65–1.58 (m, 2H, CH_2CH$_2$), 1.56–1.51 (m, 2H, CH_2CH$_2$), 1.46–1.36 (m, 2H, CH_2CH$_2$), 1.32–1.27 (m, 20H, CH_2CH$_2$ myristoyl chain), 0.90 ppm (t, ^3J(H,H) = 6.9 Hz, 3H, CH$_2$CH_3). ESI-MS (-): 489.7 $[M - H]^-$.

General procedure for the synthesis of [5-Acylamino-1-(4-methyl-2-oxo-2H-chromen-7-ylcarbamoyl)pentyl]carbamic acid benzyl esters (3a-g). 1 equiv of **2a-g** (0.09-4.53 mmol,

0.03-1.72 g) was dissolved in 52 equiv of dry pyridine (4.71-235 mmol, 0.372-18.62 g, 0.38-18.98 mL) and then 2.7 equiv of 7-amino,4-methylcoumarin (0.18-9.06 mmol, 0.03-1.60 g) were added at -15 °C. Then 2.7 equiv (0.24-12.2 mmol, 0.04-1.90 g, 0.02-1.14 mL) of $POCl_3$ were added by syringe resulting in a red-orange solution. After 40 min-3 h the mixture has been poured into a ten-fold volume of H_2O/ice and extracted with ethyl acetate (four times, 50 mL each). The combined organic layers were washed with $NaCl_{ss}$ (50 mL), 2M HCl (50 mL), $NaCl_{ss}$ (50 mL), 5% $NaHCO_3$ (50 mL) and $NaCl_{ss}$ (30 mL). The organic phase was dried over Na_2SO_4 and the solvent evaporated.

[5-Butyrylamino-1-(4-methyl-2-oxo-2H-chromen-7-ylcarbamoyl)pentyl] carbamic acid benzyl ester (3a). The resulting product was purified by flash chromatography on SiO_2 gel with DCM-methanol 96%-4%. White crystal; yield 44% (0.04 mmol, 20.1 mg); rf = 0.22 (DCM–methanol 96%-4%). ^{1}H NMR (400 MHz, $CDCl_3$): δ = 9.33 (s, 1H, N*H* amide), 7.67 (s, 1H, C*H* coumarin), 7.55 (d, ^3J(H,H) = 8.7 Hz, 1H, C*H* coumarin), 7.49 (d, ^3J(H,H) = 8.7 Hz, 1H, C*H* coumarin), 7.35 (s, 5H, C*H* benzyl), 6.18 (s, 1H, N*H* amide), 5.84 (s, 1H, N*H* amide), 5.82 (s, 1H, COC*H* coumarin), 5.13 (s, 2H, CH_2 benzyl), 4.37–4.33 (m, 1H, C*H*NH), 3.33–3.23 (m, 2H, CH_2NH), 2.41 (s, 3H, CH_3 coumarin), 2.15 (t, ^3J(H,H) = 7.5 Hz, 2H, COCH_2), 2.17–1.74 (m, 2H, CH_2CH$_2$), 1.65 (m, 2H, CH_2CH$_3$), 1.58 (quint, ^3J(H,H) = 6.1Hz, 2H, CH_2CH$_2$), 1.46 (quint, ^3J(H,H) = 6.2 Hz, 2H, CH_2CH$_2$), 0.91 ppm (t, ^3J(H,H) = 7.4 Hz, 3H, CH$_2$CH_3). ^{13}C NMR (101 MHz, $CDCl_3$): δ = 173.80 (2C, *C*O amide), 170.95 (*C*O ester), 161.17 (*C*O carbamate), 154.05 (*C*CH$_3$ coumarin), 152.32 (*C*O coumarin), 141.46 (*C*NH coumarin), 136.02 (*C*CH$_2$ benzyl), 128.50 (2C, *C*H benzyl), 128.19 (*C*H benzyl), 127.97 (2C, *C*H benzyl), 125.02 (*C*H coumarin), 115.96 (*C*H coumarin), 115.72 (*C*CH coumarin), 113.26 (*C*H coumarin), 107.19 (CO*C*H coumarin), 67.18 (*C*H$_2$ benzyl), 55.26 (*C*HNH), 38.61 (*C*H$_2$NH), 37.92 (CO*C*H$_2$), 31.05 (*C*H$_2$CH), 28.60 (C*H*$_2$CH$_2$), 22.09 (C*H*$_2$CH$_2$), 19.09 (C*C*H$_3$), 18.53 (C*H*$_2$CH$_3$), 13.69 ppm

(CH_2CH_3). HRMS (ESI): *m/z* calculated for $C_{28}H_{33}N_3O_6$ + H^+ $[M + H]^+$: 508.2442. Found: 508.2444. HPLC analysis: retention time = 19.496 min; peak area, 97%.

[5-Hexanoylamino-1-(4-methyl-2-oxo-2H-chromen-7-ylcarbamoyl)pentyl] carbamic acid benzyl ester (3b). Purification of the resulting crude product by flash chromatography on SiO_2 gel with DCM-methanol 96%-4%. Colorless powder; yield 7% (0.30 mmol, 162 mg); rf = 0.25 (DCM–methanol 96%-4%). ^{1}H NMR (400 MHz, $CDCl_3$): δ = 9.35 (s, 1H, N*H* amide), 7.68 (s, 1H, C*H* coumarin), 7.54 (d, ^3J(H,H) = 8.8 Hz, 1H, C*H* coumarin), 7.49 (d, ^3J(H,H) = 8.6 Hz, 1H, C*H* coumarin), 7.34 (s, 5H, C*H* benzyl), 6.18 (s, 1H, C*H* coumarin), 5.89 (s, 1H, COC*H*), 5.84 (d, ^3J(H,H) = 7.9 Hz, 1H, N*H* amide), 5.12 (s, 2H, CH_2 benzyl), 4.39–4.33 (m, 1H, C*H*NH), 3.36–3.19 (m, 2H, CH_2NH), 2.40 (s, 3H, CCH_3), 2.17 (t, ^3J(H,H) = 7.1 Hz, 2H, COCH_2), 2.12–1.99 (m, 2H, CH_2CH), 1.61-1.60 (m, 2H, CH_2CH$_2$), 1.60-1.57 (m, 2H, CH_2CH$_2$), 1.50-1.43 (m, 2H, CH_2CH$_2$), 1.34-1.21 (m, 4H, CH_2CH$_2$ and CH_2CH$_3$), 0.87 ppm (t, ^3J(H,H) = 6.9 Hz, 3H, CH_2CH_3). ^{13}C NMR (101 MHz, $CDCl_3$): δ = 174.10 (2C, *C*O amide), 171.11 (CO ester), 161.25 (CO carbamate), 153.97 (*C*CH_3 coumarin), 152.49 (*C*O coumarin), 141.52 (*C*NH coumarin), 136.05 (*C*CH_2 benzyl), 128.48 (2C, *C*H benzyl), 128.16 (*C*H benzyl), 127.89 (2C, *C*H benzyl), 125.01 (*C*H coumarin), 115.90 (*C*H coumarin), 115.79 (*C*CH coumarin), 113.16 (*C*H coumarin), 107.16 (CO*C*H coumarin), 67.12 (*C*H_2 benzyl), 55.35 (*C*HNH), 38.30 (*C*H_2NH), 36.58 (CO*C*H_2), 31.35 (2C, *C*H_2CH$_2$), 28.64 (*C*H_2CH$_2$), 25.42 (2C, *C*H_2CH$_2$), 22.29 (*C*H_2CH$_3$), 18.53 (C*C*H_3), 13.88 ppm (CH_2*C*H_3). HRMS (ESI): *m/z* calculated for $C_{30}H_{37}N_3O_6$ + H^+ $[M + H]^+$: 536.2755. Found: 536.2751. HPLC analysis: retention time = 22.108 min; peak area, 98%.

[5-Octanoylamino-1-(4-methyl-2-oxo-2H-chromen-7-ylcarbamoyl)pentyl] carbamic acid benzyl ester (3c). Purification by flash chromatography on SiO_2 gel with DCM-methanol 96%-4%. White crystal; yield 10% (0.39 mmol, 218 mg); rf = 0.28 (DCM–methanol 96%-4%). ^{1}H NMR (400 MHz, $CDCl_3$) δ = 9.41 (s, 1H, N*H* amide), 7.70 (s, 1H, C*H* coumarin), 7.54 (d,

^{3}J(H,H) = 8.3 Hz, 1H, C*H* coumarin), 7.49 (d, ^{3}J(H,H) = 8.3 Hz, 1H, C*H* cumarin), 7.34 (s, 5H, C*H* benzyl), 6.18 (s, 1H, N*H* amide), 6.14 (s, 1H, COC*H* coumarin), 5.87 (s, 1H, N*H* amide), 5.12 (s, 2H, CH_2 benzyl), 4.41–4.33 (m, 1H, C*H*NH), 3.34–3.23 (m, 2H, CH_2NH), 2.40 (s, 3H, CCH_3), 2.20 (t, ^{3}J(H,H) = 7.1 Hz, 2H, COCH_2), 2.08-1.73 (m, 4H, CH_2CH$_2$ and CH_2CH), 1.60 (m, 2H, CH_2CH$_2$), 1.47 (quint, ^{3}J(H,H) = 7.2 Hz, 2H, CH_2CH$_2$), 1.25 (s, 8H, CH_2CH$_2$ octanoyl chain), 0.85 ppm (t, ^{3}J(H,H) = 6.8 Hz, 3H, CH$_2$CH_3). ^{13}C NMR (101 MHz, $CDCl_3$): δ = 174.25 (2C, *C*O amide), 171.19 (*C*O ester), 161.25 (*C*CH coumarin), 153.98 (*C*O coumarin), 152.48 (*C*CH$_3$ coumarin), 141.53 (*C*NH coumarin), 136.05 (*C*O carbamate), 128.48 (2C, *C*H benzyl), 128.16 (*C*H benzyl), 127.89 (2C, *C*H benzyl), 125.00 (*C*H coumarin), 115.90 (*C*H coumarin), 115.80 (*C*CH coumarin), 113.16 (*C*H coumarin), 107.18 (CO*C*H coumarin), 67.12 (*C*H$_2$ benzyl), 55.33 (*C*HNH), 38.34 (*C*H$_2$NH), 36.55 (CO*C*H$_2$), 31.62 (*C*H$_2$CH$_2$), 31.37 (*C*H$_2$CH$_2$), 29.17 (*C*H$_2$CH), 28.92 (*C*H$_2$CH$_2$), 28.57 (*C*H$_2$CH$_2$), 25.76 (*C*H$_2$CH$_2$), 22.54 (*C*H$_2$CH$_2$), 22.25 (*C*H$_2$CH$_3$), 18.53 (C*C*H$_3$), 14.01 ppm (CH$_2$*C*H$_3$). HRMS (ESI): *m/z* calculated for $C_{32}H_{41}N_3O_6$ + Na^+ $[M + Na]^+$: 563.2888. Found: 586.2885. HPLC analysis: retention time = 24.323 min; peak area, 99%.

[5-Decanoylamino-1-(4-methyl-2-oxo-2H-chromen-7-ylcarbamoyl)pentyl] carbamic acid benzyl ester (3d). The crude product was purified by column chromatography on SiO_2 gel with DCM-methanol 96%-4%. White powder; yield 5% (0.12 mmol, 69.40 mg); rf = 0.33 (DCM–methanol 96%-4%). ^{1}H NMR (400 MHz, $CDCl_3$): δ = 9.36 (s, 1H, N*H* amide), 7.69 (s, 1H, C*H* coumarin), 7.53 (d, ^{3}J(H,H) = 8.8 Hz, 1H, C*H* coumarin), 7.49 (d, ^{3}J(H,H) = 8.6 Hz, 1H, C*H* coumarin), 7.34 (s, 5H, C*H* benzyl), 6.18 (s, 1H, N*H* amide), 5.93 (s, 1H, COC*H* coumarin), 5.85 (s, 1H, N*H* amide), 5.13 (s, 2H, CH_2 benzyl), 4.38–4.34 (m, 1H, C*H*NH), 3.33–3.23 (m, 2H, CH_2NH), 2.40 (s, 3H, CCH_3), 2.18 (t, ^{3}J(H,H) = 7.7 Hz, 2H, COCH_2), 2.07–1.87 (m, 2H, CH_2CH), 1.81–1.72 (m, 2H, CH_2CH$_2$), 1.60 (quint, ^{3}J(H,H) = 7.2 Hz, 2H, CH_2CH$_2$), 1.47 (quint,

^{3}J(H,H) = 7.2 Hz, 2H, CH_2CH$_2$), 1.23 (s, 12H, CH_2CH$_2$ deacanoyl chain), 0.86 ppm (t, ^{3}J(H,H) = 6.9 Hz, 3H, CH$_2$CH_3). ^{13}C NMR (101 MHz, $CDCl_3$): δ = 207.09 (2C, *C*O amide), 174.09 (*C*O ester), 161.24 (*C*O carbamate), 153.97 (*C*CH$_3$ coumarin), 152.47 (*C*OCH coumarin), 141.52 (*C*NH coumarin), 136.05 (*C*CH$_2$ benzyl), 128.48 (2C, *C*H benzyl), 128.16 (*C*H benzyl), 127.89 (2C, *C*H benzyl), 125.00 (*C*H coumarin), 115.90 (*C*H coumarin), 115.80 (*C*CH coumarin), 113.16 (*C*H coumarin), 107.18 (*C*H coumarin), 67.12 (*C*H$_2$ benzyl), 55.34 (*C*HNH), 38.30 (*C*H$_2$NH), 36.67 (CO*C*H$_2$), 31.80 (*C*H$_2$CH$_2$), 30.90 (*C*H$_2$CH$_2$), 29.41 (*C*H$_2$CH), 29.28 (*C*H$_2$CH$_2$), 29.24 (*C*H$_2$CH$_2$), 29.22 (*C*H$_2$CH$_2$), 28.66 (*C*H$_2$CH$_2$), 25.75 (*C*H$_2$CH$_2$), 22.60 (*C*H$_2$CH$_2$), 22.26 (*C*H$_2$CH$_3$), 18.52 (C*C*H$_3$), 14.06 ppm (CH$_2$*C*H$_3$). HRMS (ESI): *m/z* calculated for $C_{34}H_{45}N_3O_6$ + Na^+ $[M + Na]^+$: 591.3201. Found: 614.3201. HPLC analysis: retention time = 26.061 min; peak area, 99%.

[5-Lauroylamino-1-(4-methyl-2-oxo-2H-chromen-7-ylcarbamoyl)pentyl] carbamic acid benzyl ester (3e). Purification of crude product by flash column chromatography DCM–methanol (methanol gradient from 1% to 8%). White powder; yield 4% (0.04 mmol, 25 mg); rf = 0.30 (DCM–methanol 96%-4%). ^{1}H NMR (400 MHz, $CDCl_3$): δ = 9.29 (s, 1H, N*H* amide), 7.69 (s, 1H, C*H* coumarin), 7.54 (s, 1H, C*H* coumarin), 7.50 (s, 1H, C*H* coumarin), 7.35 (s, 5H, C*H* benzyl), 6.19 (s, 1H, N*H* amide), 5.80 (s, 2H, COC*H* coumarin and N*H* amide), 5.13 (s, 2H, C*H*$_2$ benzyl), 4.32-4.28 (m, 1H, C*H*NH), 3.40–3.17 (m, 2H, *C*H$_2$NH), 2.41 (s, 3H, CC*H*$_3$), 2.23-1.98 (m, 2H, C*H*$_2$CH), 1.79–1.70 (m, 4H, COC*H*$_2$ and C*H*$_2$CH$_2$), 1.61 (m, 4H, C*H*$_2$CH$_2$), 1.54–1.38 (m, 2H, C*H*$_2$CH$_2$), 1.24 (s, 14H, C*H*$_2$CH$_2$ lauroyl chain), 0.87 ppm (t, ^{3}J(H,H) = 6.8 Hz, 3H, CH$_2$C*H*$_3$). ^{13}C NMR (101 MHz, $CDCl_3$): δ = 171.26 (*C*O amide), 170.95 (*C*O amide), 161.17 (*C*O ester), 154.07 (*C*O carbamate), 152.33 (*C*NH coumarin), 141.44 (*C*O coumarin), 136.04 (*C*CH$_3$ coumarin), 128.55 (2C, *C*H benzyl), 128.22 (*C*H benzyl), 128.05 (2C, *C*H benzyl), 125.25 (*C*H coumarin), 125.12 (*C*CH coumarin), 120.65 (*C*CH$_2$ benzyl), 116.00 (*C*H coumarin), 113.31

(*C*H coumarin), 107.40 (CO*C*H coumarin), 70.04 (*C*H_2 benzyl), 67.29 (*C*HNH), 38.37 (*C*H_2NH), 37.28 (CO*C*H_2), 31.86 (*C*$H_2C H_2$), 31.36 (*C*$H_2C H_2$), 29.59 (*C*$H_2C H_2$), 29.51 (2C, *C*$H_2C H_2$), 29.38 (*C*$H_2C H_2$), 29.30 (*C*$H_2C H_2$), 28.84 (*C*$H_2C H_2$), 25.94 (*C*$H_2C H_2$), 22.64 (*C*$H_2C H_2$), 22.41 (*C*$H_2C H_2$), 18.64 (*C*H_2CH_3), 14.81 (C*C*H_3), 14.09 ppm (CH_2*C*H_3). HRMS (ESI): *m/z* calculated for $C_{36}H_{49}N_3O_6$ + Na^+ $[M + Na]^+$: 642.3514. Found: 642.3510. HPLC analysis: retention time = 25.175 min; peak area, 97%.

[5-Myristoylamino-1-(4-methyl-2-oxo-2H-chromen-7-ylcarbamoyl)pentyl] carbamic acid benzyl ester (3f). Purification of crude product by flash column chromatography DCM–methanol (methanol gradient from 1% to 10%). White powder; yield 11% (0.05mmol, 34 mg), rf = 0.32 (DCM–methanol 96%-4%). ^{1}H NMR (400 MHz, $CDCl_3$): δ = 9.56 (s, 1H, N*H* amide), 7.75 (s, 1H, C*H* coumarin), 7.57 (d, ^3J(H,H) = 8.3Hz, 1H, C*H* coumarin), 7.50 (d, ^3J(H,H) = 8.6 Hz, 1H, C*H* coumarin), 7.35 (s, 5H, C*H* benzyl), 6.89 (s, 1H, N*H* amide), 6.20 (s, 1H, COC*H*), 6.01 (s, 1H, N*H* amide), 5.12 (s, 2H, C*H*$_2$ benzyl), 4.45-4.37 (m, 1H, C*H*NH), 3.41–3.24 (m, 2H, C*H*$_2$NH), 2.4 (s, 3H, CC*H*$_3$), 2.30 (t, ^3J(H,H) = 7.3Hz, 2H, COC*H*$_2$), 2.12–1.64 (m, 2H, C*H*$_2$CH), 1.67-1.64 (m, 2H, C*H*$_2C H_2$), 1.62-1.58 (m, 2H, C*H*$_2C H_2$), 1.54-1.47 (m, 2H, C*H*$_2C H_2$), 1.33–1.23 (m, 20H, C*H*$_2C H_2$ myristoyl chain), 0.89 ppm (t, ^3J(H,H) = 6.9 Hz, 3H, CH_2C*H*$_3$). ^{13}C NMR (101 MHz, $(CD_3)_2SO$): δ = 172.40 (*C*O amide), 160.49 (*C*O amide), 156.61 (*C*O ester), 154.12 (CO carbamate), 153.55 (*C*CH_3 coumarin), 142.72 (*C*OCH coumarin), 128.81 (*C*NH coumarin), 128.28 (*C*CH_2 benzyl), 128.20 (2C, *C*H benzyl), 126.39 (*C*H benzyl), 115.71 (2C, *C*H benzyl), 115.52 (*C*H coumarin), 112.77 (*C*H coumarin), 106.15 (*C*CH coumarin), 65.95 (*C*H coumarin), 56.02 (CO*C*H coumarin), 38.53 (*C*H_2 benzyl), 35.90 (*C*HNH), 31.76 (*C*H_2NH), 29.52 (CO*C*H_2), 29.48 (*C*H_2CH), 29.40 (2C, *C*$H_2C H_2$), 29.31 (2C, *C*$H_2C H_2$), 29.20 (2C, *C*$H_2C H_2$), 29.17 (2C, *C*$H_2C H_2$), 29.12 (2C, *C*$H_2C H_2$), 25.76 (*C*$H_2C H_2$), 23.45 (*C*$H_2C H_2$), 22.56 (*C*H_2CH_3), 18.44

(C*C*H_3 coumarin), 14.42 ppm (CH_2*C*H_3). MS (ESI), *m/z*: 646.7 [M - H]$^-$. HPLC analysis: retention time = 30.424 min; peak area, 95%.

[5-Palmitoylamino-1-(4-methyl-2-oxo-2H-chromen-7-ylcarbamoyl)pentyl] carbamic acid benzyl ester (3g). Purification of crude product by flash column chromatography DCM–methanol (methanol gradient from 1% to 8%). White powder; yield 10% (0.29 mmol, 200mg); rf = 0.60 (DCM–methanol 96%-4%). ^{1}H NMR (400 MHz, $CDCl_3$): δ = 9.30 (s, 1H, N*H* amide), 7.68 (s, 1H, C*H* coumarin), 7.54 (d, ^3J(H,H) = 8.8 Hz, 1H, C*H* coumarin), 7.49 (d, ^3J = 8.6 Hz, 1H, C*H* coumarin), 7.35 (s, 5H, C*H* benzyl), 6.19 (s, 1H, N*H* amide), 5.79 (d, ^3J(H,H) = 8.8 Hz, 1H, N*H* amide), 5.75 (s, 1H, COC*H*), 5.13 (s, 2H, CH_2 benzyl), 4.38-4.30 (m, 1H, C*H*NH), 3.37-3.19 (m, 2H, CH_2NH), 2.41 (s, 3H, CCH_3), 2.16 (t, ^3J(H,H) = 7.1 Hz, 2H, COCH_2), 2.08–1.72 (m, 2H, CH_2CH$_2$), 1.64-1.60 (m, 2H, CH_2CH), 1.59-1.55 (m, 2H, CH_2CH$_2$), 1.50-1.42 (m, 2H, CH_2CH$_2$), 1.31–1.19 (m, 24H, CH_2CH$_2$ palmitoyl chain), 0.88 ppm (t, ^3J(H,H) = 6.9 Hz, 3H, CH$_2$CH_3). ^{13}C NMR (101 MHz, $CDCl_3$): δ = 174.05 (*C*O amide), 174.02 (*C*O amide), 170.98 (*C*O ester), 161.18 (*C*O carbamate), 154.04 (*C*CH_3 coumarin), 152.33 (*C*OCH coumarin), 141.47 (*C*NH coumarin), 136.03 (*C*CH$_2$ benzyl), 128.49 (2C, *C*H benzyl), 128.18 (*C*H benzyl), 127.93 (2C, *C*H benzyl), 125.00 (*C*H coumarin), 115.94 (*C*H coumarin), 115.74 (*C*CH coumarin), 113.24 (*C*H coumarin), 107.20 (CO*C*H), 67.16 (*C*H$_2$ benzyl), 65.81 (*C*HNH), 38.06 (CO*C*H$_2$), 36.71 (*C*H$_2$CH$_2$), 31.87 (*C*H$_2$CH$_2$), 31.18 (*C*H$_2$CH), 29.65 (2C, *C*H$_2$CH$_2$), 29.62 (2C, *C*H$_2$CH$_2$), 29.60 (*C*H$_2$CH$_2$), 29.48 (2C, *C*H$_2$CH$_2$), 29.31 (*C*H$_2$CH$_2$), 29.26 (*C*H$_2$CH$_2$), 28.59 (*C*H$_2$CH$_2$), 25.73 (*C*H$_2$CH$_2$), 22.64 (*C*H$_2$CH$_2$), 22.14 (*C*H$_2$CH$_2$), 18.53 (*C*H$_2$CH$_3$), 15.22 (C*C*H$_3$ coumarin), 14.08 ppm (CH$_2$*C*H$_3$). MS (ESI), *m/z*: 674.9 [M - H]$^-$. HPLC analysis: retention time = 26.635 min; peak area, 98%.

Synthesis of ethyl 2-(1-(3-fluoro-2-methylbenzyl)piperidin-3-yl)acetate (8). 2-(piperidin-3-yl) acetic acid ethyl ester (1 equiv, 5.84 mmol, 1 g) was dissolved in 2.5 mL of toluene, followed by

the addition of 2.4 equiv of triethylamine (11.7 mmol, 1.62 mL) and 1 equiv of 3-fluoro-2-methylbenzyl bromide (5.84 mmol, 1.18 g) at 0 °C. After 10 min, the mixture was warmed up to room temperature. After 18 h the precipitate was removed by filtration, washed with cyclohexane and the filtrate has been concentrated. The crude product was dried by the use of a vacuum pump for 2-5 h and then purified by flash column chromatography on SiO_2 gel with DCM-methanol (99%-1%). Colorless oil; yield 85-90% (2.45-2.89 mmol, 723-767 mg); rf = 0.67 (DCM-methanol 95%-5%). ^{1}H NMR (400 MHz, $CDCl_3$): δ = 7.10-7.0 (m, 2H, C*H* benzyl), 6.94-6.89 (m, 1H, C*H* benzyl), 4.15-4.03 (m, 2H, CH_2CH$_3$), 3.41 (s, 2H, CH_2 benzyl), 2.75-2.59 (m, 2H, CH_2COO), 2.25 (s, 3H, CH_3 benzyl), 2.24-2.22 (m, 1H, C*H* piperidine), 2.20-2.16 (m, 1H, C*H* piperidine), 2.13-1.99 (m, 1H, C*H* piperidine), 1.89-1.80 (m, 1H, C*H* piperidine), 1.76-1.74 (m, 1H, C*H* piperidine), 1.67-1.59 (m, 1H, C*H* piperidine), 1.59-1.50 (m, 2H, C*H* piperidine), 1.21 (t, ^3J(H,H) = 7.1 Hz, 3H, CH$_2$CH_3), 1.09-1.00 ppm (m, 1H, C*H* piperidine). MS (ESI), *m/z*: 294.32 $[M + H]^+$.

General procedure for the synthesis of *N*-(4-cyanophenyl)acylamide (9b-c). 1 equiv of 4-aminobenzonitrile (4.23 mmol, 500 mg) was dissolved in 15 mL of dry DCM at 0 °C under nitrogen atmosphere, followed by addition of 7 equiv of triethylamine and 4 equiv of acyl chloride. After 2 h at r.t. the reaction was quenched with water and extracted (three times, 15 mL of water each). Then the organic phase was washed with 2M HCl (once, 15 mL), $NaCl_{ss}$ (once, 15 mL), 5% Na_2CO_3 (once, 15 mL), $NaCl_{ss}$ (once, 15 mL) and dried over Na_2SO_4. The solvent was evaporated to dryness and the crude product purified by flash column chromatography on SiO_2 gel with DCM-methanol (98%-2%).

***N*-(4-cyanophenyl)octanamide (9b).** White solid; yield 62-65% (2.60-2.73 mmol, 635-666 mg); rf = 0.47 (DCM-methanol 98%-2%). ^{1}H NMR (400 MHz, $CDCl_3$): δ = 7.67 (d, ^3J(H,H) = 8.8 Hz, 2H, C*H* aromatic ring), 7.61 (d, ^3J(H,H) = 8.8 Hz, 2H, C*H* aromatic ring), 7.38 (s, 1H, N*H*

amide), 2.39 (t, ^{3}J(H,H) = 7.2 Hz, 2H, COCH_2), 1.73 (quint, ^{3}J(H,H) = 7.2 Hz, 2H, CH_2CH$_2$), 1.42–1.23 (m, 8H, CH_2CH$_2$), 0.88 ppm (t, ^{3}J(H,H) = 7.0 Hz, 3H, CH$_2$CH_3). MS (ESI), *m/z*: 243.3 $[M - H]^-$.

***N*-(4-cyanophenyl)decanamide (9c).** Yellow solid; yield 71% (5.98 mmol, 1.63 g); rf = 0.63 (DCM-methanol 99%-1%). ^{1}H NMR (400 MHz, $CDCl_3$): δ = 7.67 (d, ^{3}J(H,H) = 8.9 Hz, 2H, C*H* aromatic ring), 7.61 (d, ^{3}J(H,H) = 8.9 Hz, 2H, C*H* aromatic ring), 7.35 (s, 1H, N*H* amide), 2.39 (t, ^{3}J(H,H)= 7.6 Hz, 2H, COCH_2), 1.73 (quint, ^{3}J(H,H) = 7.6 Hz, 2H, CH_2CH$_2$), 1.39-1.27 (m, 12H, CH_2CH$_2$), 0.88 ppm (t, ^{3}J(H,H) = 6.9 Hz, 3H, CH$_2$CH_3). MS (ESI), *m/z*: 271.4 $[M - H]^-$.

General procedure for the synthesis of (Z)-*N*-(4-(*N*'-hydroxycarbamimidoyl)-phenyl)acylamide (10a-c). 1 equiv of N-(4-cyanophenyl)acylamide (3.74-5.98 mmol, 0.60-1.63 g), 3.7 equiv of $NH_2OH{\cdot}HCl$ (13.84-22.14 mmol, 0.96-1.50 g) and 1.7 equiv of Na_2CO_3 (6.36-10.17 mmol, 0.67-1.07 g) were dissolved in a mixture of water and EtOH. After stirring for 6-8 h at reflux, the reaction was cooled on ice and a yellow-orange precipitate formed. The precipitate was collected by filtration and dried under vacuum.

N-(4-(N´-hydroxycarbamimidoyl)phenyl)acetamide (10a). The reaction was performed in a mixture of 5 mL ethanol and 20 mL water. **3a** was obtained as white crystal; yield 86% (4.03 mmol, 778 mg); rf = 0.83 (DCM-methanol 80%-20%). ^{1}H NMR (400 MHz, d_6-DMSO): δ = 10.04 (s, 1H, N*H* amide), 9.53 (s, 1H, NO*H*), 7.60 (d, ^3J(H,H) = 9.1 Hz, 2H, C*H* aromatic ring), 7.56 (d, ^3J(H,H) = 9.1 Hz, 2H, C*H* aromatic ring), 5.76 (s, 2H, CNH_2), 2.05 ppm (s, 3H, COCH_3). MS (ESI), *m/z*: 194.2 $[M + H]^+$.

(Z)-N-(4-(N'-hydroxycarbamimidoyl)phenyl)octanamide (10b). A mixture of 15 mL water and 45 mL ethanol was used for the reaction. **3b** is a white crystal; yield 77% (4.04 mmol, 1.12 g); rf = 0.07 (DCM-methanol 95%-5%). ^{1}H NMR (400 MHz, d_6-DMSO): δ = 10.01 (s, 1H, N*H* amide), 9.54 (s, 1H, NO*H*), 7.86-7.23 (m, 4H, C*H* aromatic ring), 5.78 (s, 2H, CNH_2), 2.31 (t, ^3J(H,H) = 7.4 Hz, 2H, COCH_2), 1.65- 1.52 (m, 2H, CH_2CH$_2$), 1.36-1.20 (m, 8H, CH_2CH$_2$), 0.86 ppm (t, ^3J(H,H) = 6.5 Hz, 3H, CH$_2$CH_3). MS (ESI), *m/z*: 278.2 $[M + H]^+$.

(Z)-N-(4-(N'-hydroxycarbamimidoyl) phenyl)decanamide (10c). 20 mL of water and 45 mL of ethanol were used in this case as reaction solvent. **3c** is a white crystal; yield 87% (5.17 mmol, 1.58 g); rf = 0.07 (DCM-methanol 98%-2%). ^{1}H NMR (400 MHz, d_6-DMSO): δ = 9.95 (s, 1H, N*H* amide), 9.52 (s, 1H, NO*H*), 7.85-7.26 (m, 4H, C*H* aromatic ring), 5.74 (s, 2H, CNH_2), 2.30 (t, ^3J(H,H) = 7.4 Hz, 2H, COCH_2), 1.62-1.55 (quint, ^3J(H,H) = 7.3 Hz, 2H, CH_2CH$_2$), 1.33-1.19

(m, 12H, C*H*$_2$CH$_2$), 0.86 ppm (t, ^3J(H,H) = 7.1 Hz, 3H, CH$_2$C*H*$_3$). MS (ESI), *m/z*: 306.4 [M + H]$^+$.

Synthesis of *N*-(4-(5-((1-(3-fluoro-2-methylbenzyl)piperidin-3-yl)methyl)-1,2,4-oxadiazol-3-yl)phenyl)acetamide (6). 1 equiv of **8** (0.51 mmol, 150 mg), 1 equiv of **10a** (0.51 mmol, 98.8 mg) and 3.7 equiv of K_2CO_3 (1.89 mmol, 261.3mg) were mixed in 5.00 mL of pyridine and refluxed for eight hours. The reaction mixture was left for 72 h at r.t., and then was diluted with 15 mL of ethyl acetate, washed with H_2O (two times, 10 mL each) and $NaCl_{ss}$ (10 mL) and dried over Na_2SO_4. The solvent was evaporated and the crude product purified by flash column chromatography on SiO_2 gel with DCM–methanol (98%-2%). Yellow oil; yield 5% (0.03mmol, 12mg); rf= 0.28 (DCM-methanol 95%-5%). ^{1}H NMR (400 MHz, d_6-DMSO, 50°C): δ = 10.12 (s, 1H, N*H* anilide), 7.88 (d, ^3J(H,H) = 8.8 Hz, 2H, C*H* anilide), 7.75 (d, ^3J(H,H) = 8.8 Hz, 2H, C*H* anilide), 7.15-6.97 (m, 3H, C*H* benzyl), 3.44 (s, 2H, C*H*$_2$ benzyl), 3.00-2.92 (m, 2H, CHC*H*$_2$), 2.77-2.74 (m, 1H, C*H* piperidine), 2.63-2.56 (m, 1H, C*H* piperidine), 2.23 (s, 3H, CC*H*$_3$ benzyl), 2.15-2.13 (m, 1H, C*H* piperidine), 2.12-2.11 (m, 1H, C*H* piperidine), 2.09 (s, 3H, C*H*$_3$ amide), 2.00-1.92 (m, 1H, C*H* piperidine), 1.76-1.68 (m, 1H, C*H* piperidine), 1.67-1.61 (m, 1H, C*H* piperidine), 1.53-1.42 (m, 1H, C*H* piperidine), 1.21-1.11 ppm (m, 1H, C*H* piperidine). ^{13}C NMR (101 MHz, (CD$_3$)$_2$SO, 50°C): δ = 179.39 (*C*ONH amide), 169.13 (*C*N oxadiazole), 167.57 (*C*O oxadiazole), 141.18 (d, ^1J(C,F) = 264.1 Hz, *C*F), 128.14 (*C*H anilide), 126.72 (*C*H benzyl), 125.82 (*C*H benzyl), 124.27 (2C, *C*CH anilide and *C*CH$_2$ benzyl), 124.10 (*C*NH anilide), 121.02 (*C*CH$_3$ benzyl), 120.65 (*C*CH anilide), 119.49 (2C, *C*H anilide), 113.69 (*C*H benzyl), 60.53 (N*C*H$_2$ benzyl), 58.71 (N*C*H$_2$ piperidine), 53.85 (N*C*H$_2$ piperidine), 34.50 (*C*H$_2$CH piperidine), 34.47 (*C*HCH$_2$ piperidine) 30.32 (CO*C*H$_3$), 30.11 (*C*H$_2$CH piperidine), 24.50 (*C*H$_2$CH$_2$ piperidine), 10.35 ppm (C*C*H$_3$ benzyl). ^{19}F (376 MHz, (CD$_3$)$_2$SO, 50°C): δ = -117.73 ppm (s, C*F*). HRMS (ESI): *m/z* calculated for $C_{24}H_{27}FN_4O_2$ + H$^+$ [M + H]$^+$: 423.2191.

Found: 423.2195. HPLC analysis: retention time = 16.559 min; peak area, 99%.

Synthesis of *N*-(4-(5-((1-(3-fluoro-2-methylbenzyl)piperidin-3-yl)methyl)-1,2,4-oxadiazol-3-yl)phenyl)octanamide (11). 1 equiv of **8** (0.82 mmol, 240 mg), 2 equiv of **10b** (1.64 mmol, 453.5 mg) and 4 equiv of K_2CO_3 (3.27 mmol, 452 mg) in 9 mL of pyridine were mixed and the reaction was performed with microwaves (10 minutes, 180 ^oC, 300 W). Then the mixture was refluxed at 160 ^oC for 43 h, and stirred at r.t. for 12 h. After that the pyridine was removed and the reaction mixture dissolved in 40 mL of ethyl acetate, extracted with water (three times, 15 mL each), washed with $NaCl_{ss}$ (once, 15 mL) and dried over Na_2SO_4. The solvent was evaporated and the crude product purified by flash column chromatography on SiO_2 gel with DCM-methanol (98%-2%) and with DCM-methanol (95%-5%) obtaining **11** as colorless oil. Yield 28.9% (0.02 mmol,12 mg); rf = 0.36 (DCM-methanol 95%-5%). ^{1}H NMR (400 MHz, CD_3OD, 50°C): δ = 10.06 (s, 1H, N*H* anilide), 7.93 (d, ^3J(H,H) = 8.6 Hz, 2H, C*H* anilide), 7.75 (d, ^3J(H,H) = 8.6 Hz, 2H, C*H* anilide), 7.24-6.97 (m, 3H, C*H* benzyl), 3.80-3.64 (m, 2H, CH_2CH), 3.13-3.02 (m, 1H, C*H* piperidine), 3.00-2.97 (m, 1H, C*H* piperidine), 2.95-2.92 (m, 1H, C*H* piperidine), 2.44-2.42 (m, 2H, COCH_2), 2.40-2.37 (m, 1H, C*H* piperidine), 2.30 (s, 3H, CCH_3 benzyl), 2.29-2.22 (m, 1H, C*H* piperidine), 2.18 (s, 2H, CH_2 benzyl), 1.89-1.84 (m, 1H, C*H* piperidine), 1.82-1.79 (m, 1H, C*H* piperidine), 1.78-1.76 (m, 2H, CH_2CH$_2$), 1.73-1.68 (m, 2H, CH_2CH$_2$), 1.67-1.60 (m, 1H, C*H* piperidine), 1.40-1.19 (m, 7H, C*H* piperidine and CH_2CH$_2$ octanoyl chain), 0.92 ppm (t, ^3J(H,H) = 6.4 Hz, 3H, CH$_2$CH_3). ^{13}C NMR (400 MHz, CD_3OD, 50°C): δ = 178.75 (*C*ONH amide), 173.63 (*C*N oxadiazole), 167.57 (*C*O oxadiazole), 141.53 (*C*NH anilide), 127.62 (2C, *C*H anilide), 126.31 (*C*H benzyl), 126.22 (2C, *C*CH anilide and *C*CH$_2$ benzyl), 126.03 (*C*H benzyl), 120.64 (d, ^1J(C-F) = 212.6 Hz, *C*F), 119.49 (2C, *C*H anilide), 114.17 (*C*CH$_3$ benzyl), 113.94 (*C*H benzyl), 99.99 (*C*H$_2$ benzyl), 59.48 (*C*H$_2$CH), 57.74 (N*C*H$_2$ piperidine), 53.48 (N*C*H$_2$ piperidine), 36.70 (COCH$_2$), 31.49 (*C*H$_2$CH$_2$), 29.87 (*C*HCH$_2$), 29.07 (*C*H$_2$CH piperidine), 28.92 (*C*H$_2$CH$_2$),

28.77 (*C*H_2CH_2), 25.45 (*C*H_2CH_2), 23.60 (*C*H_2CH_2 piperidine), 22.28 (*C*H_2CH_3), 13.02 (CH_2*C*H_3), 9.27 ppm (C*C*H_3). ^{19}F (376 MHz, $CDCl_3$, 50°C): δ = -117.40 ppm (s, C*F*). HRMS (ESI): *m/z* calculated for $C_{30}H_{39}FN_4O_2$ + H^+ $[M + H]^+$: 507.3130. Found: 507.3129. HPLC analysis: retention time = 22.798 min; peak area, 96%.

Synthesis of *N*-(4-(5-((1-(3-fluoro-2-methylbenzyl)piperidin-3-yl)methyl)-1,2,4-oxadiazol-3-yl)phenyl)decanamide (12). 1 equiv of **8** (3.41 mmol, 1 g) was dissolved in 23 mL of ethanol followed by drop by drop addition of 4 equiv (13.63 mmol, 13.6 mL) of 1M LiOH solution. The reaction mixture was stirred for 20 h at r.t. (TLC-control), acidified with 2M HCl solution with consequent removal of water by evaporation. Under N_2 atmosphere, the previously formed carboxylic acid was dissolved in 200 µL of *N*,*N*-dimethylformamide and 2.5 mL of dry DCM. 5 equiv of $SOCl_2$ (9.31 mmol, 1.1 g) were added drop by drop at -15 °C. The reaction mixture was stirred for 3 h (TLC-control) and then $SOCl_2$ was removed by stream of N_2. 1.3 equiv of **10c** (2.42 mmol, 739 mg), solubilized in 3mL of *N*,*N*-dimethylformamide and 5 mL of dry DCM, were added to the acyl chloride, followed by 3 equiv of triethylamine (5.58 mmol, 0.77 mL). After 22 h, the solvent was evaporated and 5 mL of *N*,*N*-dimethylformamide were added. The mixture was heated at 150 °C for 3 h, basified with 2 M KOH and extracted with ethyl acetate (three times, 10 mL each), washed with $NaCl_{ss}$ (once, 10 mL) and dried over Na_2SO_4. The product was purified by flash chromatography DCM-methanol (methanol gradient from 2% to 25%) followed by preparative HPLC obtaining **12** as white powder. Yield 2.3% (0.08 mmol, 41.8 mg); rf = 0.33 (DCM-methanol 98%-2%). ^{1}H NMR (400 MHz, CD_3OD, 50°C): δ = 10.08 (s, 1H, N*H* amide), 7.90 (d, ^3J(H,H) = 8.3 Hz, 2H, C*H* anilide), 7.76 (d, ^3J(H,H) = 8.4 Hz, 2H, C*H* anilide), 7.36-7.20 (m, 3H, C*H* benzyl), 4.53-4.40 (m, 2H, CHCH_2), 3.87-3.79 (m, 1H, C*H* piperidine), 3.65-3.55 (m, 1H, C*H* piperidine), 3.16-3.12 (m, 1H, C*H* piperidine), 3.10-3.09 (m, 1H, C*H* piperidine), 3.03-3.01 (m, 1H, C*H* piperidine), 2.98-2.93 (m, 1H, C*H*

piperidine), 2.49-2.43 (m, 2H, COC*H*$_2$), 2.40 (s, 3H, CC*H*$_3$ benzyl), 2.09-1.97 (m, 3H, C*H* piperidine and C*H*$_2$ benzyl), 1.95-1.85 (m, 1H, C*H* piperidine), 1.77-1.66 (quint, ^3J(H,H) = 7.8 Hz, 2H, C*H*$_2$CH$_2$), 1.52-1.32 (m, 13H, C*H* piperidine and C*H*$_2$CH$_2$ decanoyl chain), 0.91 ppm (t, ^3J(H,H) = 6.2 Hz, 3H, CH$_2$C*H*$_3$). ^{13}C NMR (400 MHz, CD$_3$OD, 50°C): δ = 177.49 (*C*ONH amide), 173.73 (*C*N oxadiazole), 167.65 (*C*O oxadiazole), 162.77 (*C*H benzyl), 141.64 (*C*NH anilide), 127-72 (*C*CH$_3$ benzyl), 127.62 (*C*H benzyl), 127.53 (2C, *C*CH anilide and *C*CH$_2$ benzyl), 120.60 (d, ^1J(C-F) = 188.1 Hz, *C*F), 119.70 (*C*H$_2$ benzyl), 119.53 (2C, *C*H anilide), 116.57 (2C, *C*H anilide), 116.33 (*C*H benzyl), 59.34 (CH*C*H$_2$), 55.71 (N*C*H$_2$ piperidine), 52.70 (N*C*H$_2$ piperidine), 36.76 (CO*C*H$_2$), 32.37 (*C*H$_2$CH piperidine), 31.61 (*C*HCH$_2$ piperidine), 29.33 (*C*H$_2$CH$_2$), 29.18 (*C*H$_2$CH$_2$), 28.99 (*C*H$_2$CH$_2$ piperidine), 28.92 (*C*H$_2$CH$_2$ piperidine), 27.76 (*C*H$_2$CH$_2$), 25.42 (*C*H$_2$CH$_2$), 22.32 (*C*H$_2$CH$_2$), 22.18 (*C*H$_2$CH$_3$), 13.04 (CH$_2$*C*H$_3$), 9.80 ppm (C*C*H$_3$). ^{19}F (376 MHz, (CDCl$_3$, 50°C): δ = -112.65 ppm (s, C*F*). HRMS (ESI): *m/z* calculated for $C_{32}H_{43}FN_4O_2$ + H^+ $[M + H]^+$: 535.3443. Found: 535.3441. HPLC analysis: retention time = 13.378 min; peak area, 98%.

General Procedure for the Synthesis of the *N*^{7}-Substituted pyrimido[4,5-d]pyrimidine-2,4,7-triamines 7, 14-44. 2-Substituted-4-aminopyrimidin-5-carbonitriles **47** (1 equiv, 0.83 mmol) were stirred with 0.73 M free base guanidine solution in dry 2-methoxyethanol (3.5 equiv, 2.90 mmol, 3.97 mL) at 150 °C for 1.5-4.5 h. After the completion of the reaction, the mixture was concentrated, quenched with water and extracted with ethyl acetate. The organic phase was dried over anhydrous sodium sulfate, filtered and evaporated giving a crude product purified by silica gel column chromatography eluting with a mixture of chloroform/methanol/ammonia and then triturated with a mixture of petroleum ether/diethyl ether to afford the final compounds **7, 14-44** as a white powder.

N^7-(1-(4-(4-methoxyphenoxy)phenyl)ethyl)-N^7-methylpyrimido[4,5-d]pyrimidine-2,4,7-triamine (7). ^{1}H-NMR (400 MHz; d_6-DMSO) δ ppm: 1.50-1.52 (d, 3H, CHC*H*$_3$), 2.82 (br s, 3H, NC*H*$_3$), 3.74 (s, 3H, OC*H*$_3$), 6.28 (br s, 1H, C*H*CH$_3$), 6.49 (br s, 2H, C$_2$-N*H*$_2$), 6.87-6.90 (d, 2H, C*H* benzene ring), 6.94-7.00 (m, 4H, C*H* benzene rings), 7.25-7.27 (d, 2H, C*H* benzene rings), 7.41 (br s, 2H, C$_4$-N*H*$_2$), 8.95 (s, 1H, C*H* pyrimidine ring). ^{13}C-NMR (100 MHz, DMSO) δ 16.8, 29.2, 51.3, 55.9, 96.4, 115.5 (2C), 117.6 (2C), 121.1 (2C), 128.8 (2C), 136.3, 149.9, 156.0, 156.7, 157.3, 163.3, 163.4, 165.9, 166.0. MS (ESI), *m/z*: 418 $[M + H]^+$.

N^7-(1-benzylpiperidin-4-yl)pyrimido[4,5-d]pyrimidine-2,4,7-triamine (14). ^{1}H-NMR (400 MHz; d_6-DMSO) δ ppm: 1.46-1.54 (m, 2H, 2 x C*H* piperidine ring), 1.82-1.85 (m, 2H, 2 x C*H* piperidine ring), 1.99-2.04 (m, 2H, 2 x C*H* piperidine ring), 2.79-2.81 (m, 2H, 2 x C*H* piperidine ring), 3.46 (s, 2H, NC*H*$_2$Ph), 3.74 (br m, 1H, NHC$_4$-*H*-piperidine ring), 6.40 (br s, 2H, C$_2$-N*H*$_2$), 7.18-7.35 (m, 8H, C*H* benzene ring, N*H* and C$_4$-N*H*$_2$), 8.84 (s, 1H, C*H* pyrimidine ring). ^{13}C-NMR (100 MHz, DMSO) δ 31.8 (2C), 48.2, 52.8 (2C), 62.7, 96.2, 127.3, 128.6 (2C), 129.2 (2C), 139.2, 157.0, 163.3, 163.4, 165.7, 166.2. MS (ESI), *m/z*: 351 $[M + H]^+$.

7-(2-methylpiperidin-1-yl)pyrimido[4,5-d]pyrimidine-2,4-diamine (15). ^{1}H-NMR (400 MHz; DMSO) δ ppm: 1.12-1.14 (d, 3H, CHC*H*$_3$), 1.36 (m, 1H, C*H* piperidine ring), 1.58-1.70 (m, 5H, 5 x C*H* piperidine ring), 2.85-2.92 (t, 1H, C*H* piperidine ring), 4.66-4.69 (m, 1H, C*H* piperidine ring), 5.10 (br s, 1H, C*H*-CH$_3$-piperidine ring), 6.43 (br s, 2H, C$_2$-N*H*$_2$), 7.34 (br s, 2H, C$_4$-N*H*$_2$), 8.90 (s, 1H, C*H* pyrimidine ring). ^{13}C-NMR (100 MHz, DMSO) δ 15.4, 19.1, 25.9, 30.3, 38.3, 45.4, 96.1, 156.7, 162.6, 163.3, 165.9, 166.1. MS (ESI), *m/z*: 260 $[M + H]^+$.

7-(3,4-dihydroisoquinolin-2(1*H*)-yl)pyrimido[4,5-d]pyrimidine-2,4-diamine (16). ^{1}H-NMR (400 MHz; d_6-DMSO) δ ppm: 2.85-2.88 (m, 2H, C*H* piperidine ring), 4.03 (m, 2H, C*H* piperidine ring), 4.92 (s, 2H, C*H* piperidine), 6.51 (br s, 2H, C$_2$-N*H*$_2$), 7.18-7.25 (m, 4H, C*H* isoquinoline

ring), 7.43 (br s, 2H, C_4-NH_2), 8.97 (s, 1H, C*H* pyrimidine ring). ^{13}C-NMR (100 MHz, d_6-DMSO) δ 28.6, 41.6, 46.1, 96.5, 126.5, 126.7, 126.8, 129.0, 134.7, 135.4, 156.8, 162.8, 163.4, 166.0, 166.1. MS (ESI), *m/z*: 294 $[M + H]^+$.

7-(4-phenylpiperazin-1-yl)pyrimido[4,5-d]pyrimidine-2,4-diamine (17). ^{1}H-NMR (400 MHz; d_6-DMSO) δ ppm: 3.19 (m, 4H, 2 x CH_2 piperazine ring), 3.95 (m, 4H, 2 x CH_2 piperazine ring), 6.52 (br s, 2H, C_2-NH_2), 6.79.6.83 (t, 1H, C*H* benzene ring), 6.99-7.01 (m, 2H, C*H* benzene ring), 7.22-7.26 (m, 2H, C*H* benzene ring), 7.43 (br s, 2H, C_4-NH_2), 8.96 (s, 1H, C*H* pyrimidine ring). ^{13}C-NMR (100 MHz, d_6-DMSO) δ 43.7 (2C), 48.9 (2C), 96.6, 116.3 (2C), 119.6, 129.4 (2C), 151.5, 156.8, 162.8, 163.4, 166.0, 166.1. MS (ESI), *m/z*: 323 $[M + H]^+$.

***N*^{7}-(4-methoxybenzyl)pyrimido[4,5-d]pyrimidine-2,4,7-triamine (18).** ^{1}H-NMR (400 MHz; d_6-DMSO) δ ppm: 3.71 (s, 3H, OCH_3), 4.42 (br m, 2H, NHCH_2Ph), 6.46 (br s, 2H, C_2-NH_2), 6.84-6.86 (d, 2H, C*H* benzene ring), 7.24-7.31 (br m, 4H, 2 x C*H* benzene ring and C_4-NH_2), 7.66-7.76 (br m, 1H, N*H*CH_2Ph), 8.86 (s, 1H, C*H* pyrimidine ring). ^{13}C-NMR (100 MHz, d_6-DMSO) δ 43.7, 55.5, 96.4, 113.9 (2C), 129.0 (2C), 132.8, 157.0, 158.5, 163.3, 164.1, 165.9, 166.3. MS (ESI), *m/z*: 298 $[M + H]^+$.

***N*^{7}-(1-phenylethyl)pyrimido[4,5-d]pyrimidine-2,4,7-triamine (19).** ^{1}H-NMR (400 MHz; d_6-DMSO) δ ppm: 1.41-1.43 (d, 3H, CHCH_3), 5.14 (br s, 1H, C*H*CH_3), 6.44 (br s, 2H, C_2-NH_2), 7.16-7.19 (m, 1H, C*H* benzene ring), 7.27-7.39 (m, 6H, 4 x C*H* benzene ring and C_4-NH_2), 7.79 (br m, 1H, N*H*), 8.85 (s, 1H, C*H* pyrimidine ring). ^{13}C-NMR (100 MHz, d_6-DMSO) δ 23.4, 50.0, 96.4, 126.5 (2C), 126.8, 128.5 (2C), 146.2, 156.9, 163.3, 163.4, 165.9, 166.2. MS (ESI), *m/z*: 282 $[M + H]^+$.

N^7-benzyl-N^7-methylpyrimido[4,5-d]pyrimidine-2,4,7-triamine (20). ^{1}H-NMR (400 MHz; d_6-DMSO) δ ppm: 3.09 (s, 3H, NCH_3), 4.89 (s, 2H, CH_2Ph), 6.49 (br s, 2H, C_2-NH_2), 6.24-7.33 (m, 7H, 5 x C*H* benzene ring and C_4-NH_2), 8.94 (s, 1H, C*H* pyrimidine ring). ^{13}C-NMR (100 MHz, d_6-DMSO) δ 35.1, 51.9, 96.4, 127.3 (2C), 127.7, 128.9 (2C), 139.0, 156.8, 163.4, 163.6, 166.0, 166.1. MS (ESI), *m/z*: 282 $[M + H]^+$.

N^7-methyl-N^7-(1-phenylethyl)pyrimido[4,5-d]pyrimidine-2,4,7-triamine (21). ^{1}H-NMR (400 MHz; d_6-DMSO) δ ppm: 1.53-1.55 (d, 3H, CHCH_3), 2.82 (s, 3H, NCH_3), 6.30 (br m, 1H, C*H*CH_3), 6.48 (br s, 2H, C_2-NH_2), 7.28-7.34 (m, 7H, 5 x C*H* benzene ring and C_4-NH_2), 8.96 (s, 1H, C*H* pyrimidine ring). ^{13}C-NMR (100 MHz, d_6-DMSO) δ 16.7, 29.3, 51.8, 96.4, 127.2 (2C), 127.3, 128.8 (2C), 142.2, 156.7, 163.4, 163.4, 165.9, 166.0. MS (ESI), *m/z*: 296 $[M + H]^+$.

N^7-(1-(4-methoxyphenyl)ethyl)-N^7-methylpyrimido[4,5-d]pyrimidine-2,4,7-triamine (22). ^{1}H-NMR (400 MHz; d_6-DMSO) δ ppm: 1.49 (d, 3H, CHCH_3), 2.78 (s, 3H, NCH_3), 3.73 (s, 3H, OCH_3), 6.26 (br s, 1H, C*H*CH_3), 6.48 (br s, 2H, C_2-NH_2), 6.88-6.90 (d, 2H, C*H* benzene ring), 7.20-7.22 (d, 2H, C*H* benzene ring), 7.39 (br s, 2H, C_4-NH_2), 8.95 (s, 1H, C*H* pyrimidine ring). ^{13}C-NMR (100 MHz, d_6-DMSO) δ 16.8, 29.1, 51.2, 55.5, 96.4, 114.2 (2C), 128.4 (2C), 134.0, 156.7, 158.6, 163.3, 163.4, 166.0, 166.1. MS (ESI), *m/z*: 326 $[M + H]^+$.

N^7-(1-([1,1'-biphenyl]-4-yl)ethyl)-N^7-methylpyrimido[4,5-d]pyrimidine-2,4,7-triamine (23). ^{1}H-NMR (400 MHz; d_6-DMSO) δ ppm: 1.57-1.59 (d, 3H, CHCH_3), 2.87 (s, 3H, NCH_3), 6.35 (br s, 1H, C*H*CH_3), 6.51 (br s, 2H, C_2-NH_2), 7.34-7.48 (m, 7H, 5 x C*H* benzene rings and C_4-NH_2), 7.63-7.66 (m, 4H, C*H* benzene rings), 8.97 (s, 1H, C*H* pyrimidine ring). ^{13}C-NMR (100 MHz, d_6-DMSO) δ 16.9, 29.4, 51.7, 96.5, 127.0 (2C), 127.1 (2C), 127.8 (2C), 127.9, 129.4 (2C), 139.2, 140.3, 141.5, 156.7, 163.4, 163.4, 166.0, 166.1. MS (ESI), *m/z*: 372 $[M + H]^+$.

N^7-methyl-N^7-(1-(4-phenoxyphenyl)ethyl)pyrimido[4,5-d]pyrimidine-2,4,7-triamine (24). ^{1}H-NMR (400 MHz; d_6-DMSO) δ ppm: 1.52-1.54 (d, 3H, CHC*H*$_3$), 2.84 (s, 3H, NC*H*$_3$), 6.30 (br s, 1H, C*H*CH$_3$), 6.49 (br s, 2H, C$_2$-N*H*$_2$), 6.97-7.01 (m, 4H, C*H* benzene rings), 7.11-7.15 (t, 1H, C*H* benzene ring), 7.30-7.40 (m, 6H, C*H* benzene rings and C$_4$-N*H*$_2$), 8.96 (s, 1H, C*H* pyrimidine ring). ^{13}C-NMR (100 MHz, d_6-DMSO) δ 16.8, 29.2, 51.4, 96.5, 118.9 (2C), 119.0 (2C), 123.8, 128.9 (2C), 130.5 (2C), 137.3, 155.9, 156.7, 157.2, 163.3, 163.4, 166.0, 166.1. MS (ESI), *m/z*: 388 $[M + H]^+$.

N^7-(1-(4-(4-methoxyphenoxy)phenyl)ethyl)pyrimido[4,5-d]pyrimidine-2,4,7-triamine (25). ^{1}H-NMR (400 MHz; d_6-DMSO) δ ppm: 1.40-1.42 (d, 3H, CHC*H*$_3$), 3.91 (s, 3H, OC*H*$_3$), 5.12 (br m, 1H, C*H*CH$_3$), 6.45 (br s, 2H, C$_2$-N*H*$_2$), 6.83-6.85 (m, 2H, C*H* benzene rings), 6.92-6.98 (m, 4H, C*H* benzene rings), 7.20-7.36 (m, 4H, C*H* benzene rings and C$_4$-N*H*$_2$), 7.76-7.78 (br m, 1H, N*H*), 8.85 (s, 1H, C*H* pyrimidine ring). ^{13}C-NMR (100 MHz, d_6-DMSO) δ 23.3, 49.4, 55.9, 96.4, 115.5 (2C), 117.5 (2C), 121.0 (2C), 128.0 (2C), 140.4, 150.1, 155.9, 156.9, 157.0, 163.3, 163.6, 165.9, 166.2. MS (ESI), *m/z*: 404 $[M + H]^+$.

N^7-(4-(4-methoxyphenoxy)benzyl)-N^7-methylpyrimido[4,5-d]pyrimidine-2,4,7-triamine (26). Yield: 68.0 %. ^{1}H-NMR (400 MHz; d_6-DMSO) δ ppm: 3.08 (br s, 3H, NC*H*$_3$), 3.74 (s, 3H, OC*H*$_3$), 4.85 (s, 2H, N(CH$_3$)C*H*$_2$Ph), 6.50 (br s, 2H, C$_2$-N*H*$_2$), 6.86-6.88 (d, 2H, C*H* benzene rings), 6.93-6.99 (m, 4H, C*H* benzene rings), 7.23 (br m, 2H, C*H* benzene rings), 7.41 (br s, 2H, C$_4$-N*H*$_2$), 8.94 (s, 1H, C*H* pyrimidine ring). ^{13}C-NMR (100 MHz, d_6-DMSO) δ 35.0, 51.3, 55.9, 96.4, 115.5 (2C), 117.8 (2C), 121.0 (2C), 129.3 (2C), 133.2, 150.0, 156.0, 156.7, 157.4, 163.4, 163.5, 166.0, 166.1. MS (ESI), m/z: 404 $[M + H]^+$.

N^7-(1-(4-(4-methoxyphenoxy)phenyl)propyl)-N_7-methylpyrimido[4,5-d]pyrimidine-2,4,7-triamine (27). ^{1}H-NMR (400 MHz; d_6-DMSO) δ ppm: 0.85 (t, 3H, CH$_2$C*H*$_3$), 1.90-2.07 (m, 2H,

C*H*$_2$CH$_3$), 2.79-2.82 (br s, 3H, NC*H*$_3$), 3.74 (s, 3H, OC*H*$_3$), 6.10 (br m, 1H, C*H*CH$_3$), 6.48 (br s, 2H, C$_2$-N*H*$_2$), 6.86-6.88 (m, 2H, C*H* benzene rings), 6.93-7.00 (m, 4H, C*H* benzene rings), 7.20-7.38 (br m, 4H, C*H* benzene rings and C$_4$-N*H*$_2$), 8.94 (s, 1H, C*H* pyrimidine ring). ^{13}C -NMR (100 MHz, d_6-DMSO) δ 11.5, 23.5, 28.9, 55.9, 57.2, 96.3, 115.5 (2C), 117.5 (2C), 121.1 (2C), 129.1 (2C), 135.6, 149.9, 156.1, 156.5, 157.4, 163.4, 164.0, 166.0, 166.1. MS (ESI), *m/z*: 432 [M + H]$^+$.

***N*^{7}-(1-(4-(4-methoxyphenoxy)phenyl)-2-methylpropyl)-*N*^{7}-methylpyrimido[4,5-d]pyrimidine-2,4,7-triamine (28).** ^{1}H-NMR (400 MHz; d_6-DMSO) (mixture of two rotamers 50:50) δ ppm: 0.83 and 0.89 (two d, 6H, CH(C*H*$_3$)$_2$), 2.51-2.58 (m, 1H, C*H*(CH$_3$)$_2$), 2.81 and2.89 (two br s, 3H, NC*H*$_3$), 3.74 (s, 3H, OC*H*$_3$), 5.82-5.84 (m, 1H, C*H*CH(C*H*$_3$)$_2$), 6.46 (two br s, 2H, C$_2$-N*H*$_2$), 6.86-6.88 (m, 2H, C*H* benzene rings), 6.93-7.01 (m, 4H, C*H* benzene rings), 7.36-7.42 (m, 4H, 2 x C*H* benzene rings and C$_4$-N*H*$_2$), 8.91 and 8.95 (two s, 1H, C*H* pyrimidine ring). ^{13}C -NMR (100 MHz, d_6-DMSO) δ 20.0 (2C), 21.0, 27.6, 28.9, 55.9, 96.2, 115.5 (2C), 117.4 (2C), 121.3 (2C), 130.1 (2C), 134.4, 149.7, 156.1, 156.2, 156.8, 157.5, 163.3, 163.7, 166.0. MS (ESI), *m/z*: 446 [M + H]$^+$.

***N*^{7}-((4-(4-methoxyphenoxy)phenyl)(phenyl)methyl)-*N*^{7}-methylpyrimido[4,5-d]pyrimidine-2,4,7-triamine (29).** ^{1}H-NMR (400 MHz; d_6-DMSO) δ ppm: 2.89 (br s, 3H, NC*H*$_3$), 3.93 (s, 3H, OC*H*$_3$), 6.52 (br s, 2H, C$_2$-N*H*$_2$), 6.91-7.04 (m, 6H, C*H* benzene rings), 7.13-7.18 (m, 4H, C*H* benzene rings), 7.28-7.43 (m, 6H, 4 x C*H* benzene rings and C$_4$-N*H*$_2$), 8.97 (m, 1H, C*H* pyrimidine ring). ^{13}C-NMR (100 MHz, d_6-DMSO) δ 32.0, 55.9, 61.2, 96.8, 115.6 (2C), 117.6 (2C), 121.3 (2C), 127.6, 128.7 (2C), 128.9 (2C), 130.5 (2C), 134.4, 140.5, 149.7, 156.2, 156.7, 157.6, 163.4, 163.6, 166.0, 166.1. MS (ESI), *m/z*: 480 [M + H]$^+$.

N^7-(1-(4-(3-methoxyphenoxy)phenyl)ethyl)-N^7-methylpyrimido[4,5-d]pyrimidine-2,4,7-triamine (30). ^{1}H-NMR (400 MHz; d_6-DMSO) δ ppm: 1.52-1.54 (d, 3H, CHC*H*$_3$), 2.83 (br s, 3H, NC*H*$_3$), 3.73 (s, 3H, OC*H*$_3$), 6.31 (br s, 1H, C*H*CH$_3$), 6.49-6.54 (br m, 3H, C*H* benzene rings and C$_2$-N*H*$_2$), 6.58 (t, 1H, C*H* benzene ring), 6.69-6.72 (dd, 1H, C*H* benzene ring), 6.98-7.00 (d, 2H, C*H* benzene rings), 7.25-7.32 (m, 3H, C*H* benzene rings), 7.40 (br s, 2H, C$_4$-N*H*$_2$), 8.96 (s, 1H, C*H* pyrimidine ring). ^{13}C-NMR (100 MHz, d_6-DMSO) δ 16.8, 29.2, 51.4, 55.7, 96.5, 100.0, 105.0, 109.5, 110.8, 119.1 (2C), 128.9, 130.9 (2C), 137.4, 155.7, 156.7, 158.4, 161.2, 163.3, 163.4, 166.0. MS (ESI), *m/z*: 418 $[M + H]^+$.

N^7-(1-(4-(3,4-dimethoxyphenoxy)phenyl)ethyl)-N^7-methylpyrimido[4,5-d]pyrimidine-2,4,7-triamine (31). ^{1}H-NMR (400 MHz; d_6-DMSO) δ ppm: 1.50-1.52 (d, 3H, CHC*H*$_3$), 2.82 (br s, 3H, NC*H*$_3$), 3.72 (s, 3H, OC*H*$_3$), 3.74 (s, 3H, OC*H*$_3$), 6.29 (br s, 1H, C*H*CH$_3$), 6.48-6.53 (br m, 3H, C*H* benzene ring and C$_2$-N*H*$_2$), 6.74 (d, 1H, C*H* benzene ring), 6.89-6.95 (m, 3H, C*H* benzene rings), 7.25-7.27 (m, 2H, C*H* benzene rings), 7.40 (br s, 2H, C$_4$-N*H*$_2$), 8.96 (s, 1H, C*H* pyrimidine ring). ^{13}C-NMR (100 MHz, d_6-DMSO) δ 16.9, 29.2, 51.3, 56.1, 56.4, 96.5, 105.3, 110.9, 113.0, 117.6 (2C), 128.7 (2C), 136.3, 145.8, 150.1, 150.3, 156.7, 157.2, 163.3, 163.4, 166.0, 166.1. MS (ESI), *m/z*: 448 $[M + H]^+$.

N^7-(1-(4-(3,5-dimethoxyphenoxy)phenyl)ethyl)-N^7-methylpyrimido[4,5-d]pyrimidine-2,4,7-triamine (32). ^{1}H-NMR (400 MHz; d_6-DMSO) δ ppm: 1.52-1.54 (d, 3H, CHC*H*$_3$), 2.83 (br s, 3H, NC*H*$_3$), 3.70 (s, 6H, 2 x OC*H*$_3$), 6.13 (m, 2H, C*H* benzene rings), 6.28 (m, 2H, C*H*CH$_3$ and C*H* benzene ring), 6.48 (br s, 2H, C$_2$-N*H*$_2$), 6.99 (d, 2H, C*H* benzene rings), 7.29-7.40 (m, 4H, 2 x C*H* benzene rings and C$_4$-N*H*$_2$), 8.96 (s, 1H, C*H* pyrimidine ring). ^{13}C-NMR (100 MHz, d_6-DMSO) δ 16.8, 29.2, 51.4, 55.8 (2C), 95.9, 96.5, 97.5 (2C), 119.2 (2C), 128.9 (2C), 137.5, 155.5, 156.7, 159.0, 161.8 (2C), 163.3, 163.4, 166.0, 166.1. MS (ESI), *m/z*: 448 $[M + H]^+$.

N^7-((4-(3,5-dimethoxyphenoxy)phenyl)(phenyl)methyl)-N^7-methylpyrimido[4,5-d]pyrimidine-2,4,7-triamine (33). ^{1}H-NMR (400 MHz; d_6-DMSO) δ ppm: 2.91 (br s, 3H, NC*H*$_3$), 3.71 (s, 6H, 2 x OC*H*$_3$), 6.17 (d, 2H, C*H* benzene rings), 6.30 (t, 1H, C*H* benzene rings), 6.52 (br s, 2H, C$_2$-N*H*$_2$), 7.02-7.04 (d, 2H, C*H* benzene rings), 7.17-7.20 (m, 4H, C*H* benzene rings), 7.29-7.46 (m, 6H, C*H* benzene rings, C*H*Ph and C$_4$-N*H*$_2$), 8.98 (s, 1H, C*H* pyrimidine ring). ^{13}C-NMR (100 MHz, d_6-DMSO) δ 32.0, 55.8 (2C), 61.2, 96.0, 97.8 (2C), 119.1 (2C), 119.1, 127.6, 128.7 (2C), 129.0 (2C), 130.5 (2C), 135.5, 140.5, 155.9, 156.8, 158.8, 161.9 (2C), 162.0, 163.4, 163.6, 166.1. MS (ESI), *m/z*: 510 $[M + H]^+$.

N^7-(1-(4-(3,4,5-trimethoxyphenoxy)phenyl)ethyl)-N^7-methylpyrimido[4,5-d]pyrimidine-2,4,7-triamine (34). ^{1}H-NMR (400 MHz; d_6-DMSO) δ ppm: 1.51-1.53 (d, 3H, CHC*H*$_3$), 2.82 (br s, 3H, NC*H*$_3$), 3.64 (s, 3H, OC*H*$_3$), 3.71 (s, 6H, 2 x OC*H*$_3$), 6.30 (br s, 1H, C*H*CH$_3$), 6.37 (s, 2H, C*H* benzene ring), 6.48 (br s, 2H, C$_2$-N*H*$_2$), 6.94-6.96 (d, 2H, C*H* benzene ring), 7.27-7.29 (d, 2H, C*H* benzene ring) 7.40 (br s, 2H, C$_4$-N*H*$_2$), 8.96 (s, 1H, C*H* pyrimidine ring). ^{13}C-NMR (100 MHz, d_6-DMSO) δ 16.9, 29.2, 51.3, 56.4 (2C), 60.6, 96.5, 97.8 (2C), 117.9 (2C), 128.8 (2C), 134.4, 136.7, 152.6, 154.1, 156.6, 156.7 (2C), 163.3, 163.4, 166.0, 166.1. MS (ESI), *m/z*: 478 $[M + H]^+$.

N^7-methyl-N^7-(1-(4-(4-(trifluoromethoxy)phenoxy)phenyl)ethyl)pyrimido[4,5-d]pyrimidine-2,4,7-triamine (35). ^{1}H-NMR (400 MHz; d_6-DMSO) δ ppm: 1.53-1.55 (d, 3H, CHC*H*$_3$), 2.85 (br s, 3H, NC*H*$_3$), 6.31 (br s, 1H, C*H*CH$_3$), 6.49 (br s, 2H, C$_2$-N*H*$_2$), 7.03-7.10 (m, 4H, C*H* benzene ring), 7.33-7.39 (m, 6H, C*H* benzene ring and C$_4$-N*H*$_2$), 8.96 (s, 1H, C*H* pyrimidine ring). ^{13}C-NMR (100 MHz, d_6-DMSO) δ 16.9, 29.2, 51.4, 96.5, 119.5 (2C), 120.0 (2C), 120.6 (q OCF_3), 123.4 (2C), 129.1 (2C), 138.0, 144.0, 155.3, 156.3, 156.7, 163.3, 163.4, 166.0, 166.1. MS (ESI), *m/z*: 472 $[M + H]^+$.

N^7-methyl-N^7-(1-(4-(4-(methylthio)phenoxy)phenyl)ethyl)pyrimido[4,5-d]pyrimidine-2,4,7-triamine (36). ^{1}H-NMR (400 MHz; d_6-DMSO) δ ppm: 1.52-1.54 (d, 3H, CHC*H*$_3$), 2.46 (s, 3H, SC*H*$_3$), 2.83 (br s, 3H, NC*H*$_3$), 6.30 (br m, 1H, C*H*CH$_3$), 6.48 (br s, 2H, C$_2$-N*H*$_2$), 6.96-7.00 (m, 4H, C*H* benzene rings), 7.28-7.31 (m, 4H, C*H* benzene rings), 7.39 (br s, 2H C$_4$-N*H*$_2$), 8.95 (s, 1H, C*H* pyrimidine ring). ^{13}C-NMR (100 MHz, d_6-DMSO) δ 16.2, 16.9, 29.2, 51.4, 96.5, 118.7 (2C), 119.9 (2C), 128.9 (2C), 128.9 (2C), 132.7, 137.2, 154.9, 156.0, 156.7, 163.3, 163.4, 166.0, 166.1. MS (ESI), *m/z*: 434 $[M + H]^+$.

N^7-(1-(4-(4-(benzyloxy)phenoxy)phenyl)ethyl)-N^7-methylpyrimido[4,5-d]pyrimidine-2,4,7-triamine (37). ^{1}H-NMR (400 MHz; d_6-DMSO) δ ppm: 1.50-1.52 (d, 3H, CHC*H*$_3$), 2.82 (br s, 3H, NC*H*$_3$), 5.08 (s, 2H, OC*H*$_2$Ph), 6.28 (br s, 1H, C*H*CH$_3$), 6.48 (br s, 2H, C$_2$-N*H*$_2$), 6.88-6.90 (d, 2H, CH benzene rings), 6.98-7.05 (m, 4H, C*H* benzene rings), 7.26-7.28 (d, 2H, C*H* benzene rings), 7.34-7.47 (m, 7H, 5 x C*H* benzene rings and C$_4$-N*H*$_2$), 8.96 (s, 1H, C*H* pyrimidine ring). ^{13}C-NMR (100 MHz, d_6-DMSO) δ 16.9, 29.2, 51.3, 70.1, 96.5, 116.5 (2C), 117.7 (2C), 121.0 (2C), 128.2 (2C), 128.3 (2C), 128.8, 128.9 (2C), 136.4, 137.5, 150.1, 155.1, 156.7, 157.2, 163.3, 163.4, 166.0, 166.1. MS (ESI), *m/z*: 494 $[M + H]^+$.

N^7-(1-(4-((4-methoxynaphthalen-1-yl)oxy)phenyl)ethyl)-N^7-methylpyrimido[4,5-d]pyrimidine-2,4,7-triamine (38). ^{1}H-NMR (400 MHz; d_6-DMSO) δ ppm: 1.49-1.51 (d, 3H, CHC*H*$_3$), 2.82 (br s, 3H, NC*H*$_3$), 3.98 (s, 3H, OC*H*$_3$), 6.28 (br s, 1H, C*H*CH$_3$), 6.46 (br s, 2H, C$_2$-N*H*$_2$), 6.89-6.96 (m, 3H, CH aromatic rings), 7.07-7.09 (d, 1H, C*H* naphthalene ring), 7.25-7.27 (d, 2H, C*H* aromatic rings), 7.38 (br s, 2H, C$_4$-N*H*$_2$), 7.53-7.58 (m, 2H, C*H* naphthalene ring), 7.89-7.91 (m, 1H, C*H* naphthalene ring), 8.19-8.21 (m, 1H, C*H* naphthalene ring), 8.95 (s, 1H, C*H* pyrimidine ring). ^{13}C-NMR (100 MHz, d_6-DMSO) δ 16.9, 29.2, 51.3, 56.2, 96.4, 104.5,

116.3, 116.9 (2C), 121.9, 122.4, 126.3, 126.5, 127.4, 127.6, 128.8 (2C), 136.2, 144.9, 152.1, 156.7, 158.0, 163.3, 163.4, 166.0, 166.1. MS (ESI), *m/z*: 468 $[M + H]^+$.

***N*^{7}-(1-(4-((4-methoxybenzyl)oxy)phenyl)ethyl)-*N*^{7}-methylpyrimido[4,5-d]pyrimidine-2,4,7-triamine (39).** ^{1}H-NMR (400 MHz; d_6-DMSO) δ ppm: 1.48-1.50 (d, 3H, CHC*H*$_3$), 2.79 (br s, 3H, NC*H*$_3$), 3.75 (s, 3H, OC*H*$_3$), 4.99 (s, 2H, OC*H*$_2$Ph), 6.26 (br s, 1H, C*H*CH$_3$), 6.47 (br s, 2H, C$_2$-N*H*$_2$), 6.93-6.97 (m, 4H, CH benzene rings), 7.20-7.22 (d, 2H, C*H* benzene rings), 7.36-7.38 (m, 4H, 2 x C*H* benzene rings and C$_4$-N*H*$_2$), 8.95 (s, 1H, C*H* pyrimidine ring). ^{13}C-NMR (100 MHz, d_6-DMSO) δ 16.8, 29.1, 51.2, 55.5, 69.4, 96.4, 114.3 (2C), 115.0 (2C), 128.4 (2C), 129.4, 129.9 (2C), 134.2, 156.7, 157.8, 159.4, 163.3, 163.4, 166.0, 166.1. MS (ESI), *m/z*: 432 $[M + H]^+$.

***N*^{7}-(1-(4-((4-methoxyphenyl)thio)phenyl)ethyl)-*N*^{7}-methylpyrimido[4,5-d]pyrimidine-2,4,7-triamine (40).** ^{1}H-NMR (400 MHz; d_6-DMSO) δ ppm: 1.48-1.50 (d, 3H, CHC*H*$_3$), 2.81 (br s, 3H, NC*H*$_3$), 3.77 (s, 3H, OC*H*$_3$), 6.24 (br s, 1H, C*H*CH$_3$), 6.49 (br s, 2H, C$_2$-N*H*$_2$), 6.98-7.01 (d, 2H, CH benzene rings), 7.10-7.12 (d, 2H, C*H* benzene rings), 7.21-7.41 (m, 6H, 4 x C*H* benzene rings and C$_4$-N*H*$_2$), 8.94 (s, 1H, C*H* pyrimidine ring). ^{13}C-NMR (100 MHz, d_6-DMSO) δ 16.8, 29.3, 51.5, 55.8, 96.5, 115.8 (2C), 123.8, 128.2 (2C), 128.6 (2C), 135.5 (2C), 136.4, 140.4, 156.7, 160.1, 163.3, 163.4, 166.0, 166.1. MS (ESI), *m/z*: 434 $[M + H]^+$.

***N*^{7}-(1-(4-((3,5-dimethoxyphenyl)thio)phenyl)ethyl)-*N*^{7}-methylpyrimido[4,5-d]pyrimidine-2,4,7-triamine (41).** ^{1}H-NMR (400 MHz; d_6-DMSO) δ ppm: 1.53-1.55 (d, 3H, CHC*H*$_3$), 2.83 (br s, 3H, NC*H*$_3$), 3.69 (s, 6H, 2 x OC*H*$_3$), 6.30 (br s, 1H, C*H*CH$_3$), 6.36 (m, 2H, C*H* benzene ring), 6.41 (m, 1H, C*H* benzene ring), 6.50 (br s, 2H, C$_2$-N*H*$_2$), 7.31-7.38 (m, 6H, 4 x C*H* benzene ring and C$_4$-N*H*$_2$), 8.96 (s, 1H, C*H* pyrimidine ring). ^{13}C-NMR (100 MHz, d_6-DMSO) δ 16.7, 29.4, 51.6, 55.8 (2C), 96.5, 99.4, 107.9 (2C), 128.5 (2C), 132.3, 132.3 (2C), 138.0, 142.4, 156.7, 161.3 (2C), 163.4, 166.0, 166.1, 166.2. MS (ESI), *m/z*: 464 $[M + H]^+$.

***N*^{7}-((4-((3,5-dimethoxyphenyl)thio)phenyl)(phenyl)methyl)-*N*^{7}-methylpyrimido[4,5-d]pyrimidine-2,4,7-triamine (42).** ^{1}H-NMR (400 MHz; d_6-DMSO) δ ppm: 2.90 (br s, 3H, NC*H*$_3$), 3.70 (s, 6H, 2 x OC*H*$_3$), 6.42 (m, 3H, C*H* benzene rings), 6.53 (br s, 2H, C_2-N*H*$_2$), 7.17-7.21 (m, 4H, C*H* benzene rings), 7.30-7.34 (m, 1H, C*H* benzene ring), 7.37-7.46 (m, 7H, C*H* benzene rings, C*H*Ph and C_4-N*H*$_2$), 8.97 (s, 1H, C*H* pyrimidine ring). ^{13}C-NMR (100 MHz, d_6-DMSO) δ 32.1, 55.8 (2C), 61.5, 96.9, 99.7, 108.3 (2C), 127.8, 128.9 (2C), 129.0 (2C), 130.0 (2C), 132.0 (2C), 133.0, 137.5, 140.1, 140.3, 156.8, 161.4 (2C), 163.4, 163.5, 166.1, 166.2. MS (ESI), *m/z*: 526 $[M + H]^+$.

***N*$_7$-(1-(4-((4-methoxyphenyl)amino)phenyl)ethyl)-*N*$_7$-methylpyrimido[4,5-d]pyrimidine-2,4,7-triamine (43).** ^{1}H-NMR (400 MHz; d_6-DMSO) δ ppm: 1.46-1.48 (d, 3H, CHC*H*$_3$), 2.79 (br s, 3H, NC*H*$_3$), 3.71 (s, 3H, OC*H*$_3$), 6.23 (br s, 1H, C*H*CH$_3$), 6.46 (br s, 2H, C_2-N*H*$_2$), 6.84-6.90 (m, 4H, CH benzene rings), 7.01-7.03 (d, 2H, C*H* benzene rings), 7.09-7.11 (m, 2H, C*H* benzene rings), 7.38 (br s, 2H, C_4-N*H*$_2$), 7.83 (s, 1H, N*H*Ph-OCH$_3$), 8.95 (s, 1H, C*H* pyrimidine ring). ^{13}C-NMR (100 MHz, d_6-DMSO) δ 16.7, 29.1, 51.3, 55.7, 96.3, 115.0 (2C), 115.2 (2C), 120.6 (2C), 128.2 (2C), 131.7, 136.7, 144.4, 154.1, 156.7, 163.3, 163.4, 166.0, 166.1. MS (ESI), *m/z*: 417 $[M + H]^+$.

***N*-(4-(1-((5,7-diaminopyrimido[4,5-d]pyrimidin-2-yl)(methyl)amino)ethyl)phenyl)-4-methoxybenzamide (44).** ^{1}H-NMR (400 MHz; d_6-DMSO) δ ppm: 1.51-1.53 (d, 3H, CHC*H*$_3$), 2.81 (br s, 3H, NC*H*$_3$), 3.83 (s, 3H, OC*H*$_3$), 6.30 (br m, 1H, C*H*CH$_3$), 6.46 (br s, 2H, C_2-N*H*$_2$), 7.04-7.06 (d, 2H, C*H* benzene ring), 7.24-7.26 (d, 2H, C*H* benzene ring), 7.38 (br s, 2H, C_4-N*H*$_2$), 7.71-7.73 (d, 2H, C*H* benzene ring), 7.94-7.96 (d, 2H, C*H* benzene ring), 8.96 (s, 1H, C*H* pyrimidine ring), 10.08 (s, 1H, N*H*CO). ^{13}C-NMR (100 MHz, d_6-DMSO) δ 16.7, 29.2, 51.5, 55.9,

96.4, 114.0 (2C), 120.7 (2C), 127.4, 127.5 (2C), 130.0 (2C), 137.1, 138.6, 156.7, 162.3, 163.3, 163.4, 165.3, 166.0, 166.1. MS (ESI), *m/z*: 445 $[M + H]^+$.

General Procedure for the Synthesis of the Intermediate Ketones 45f-q, s-u. A mixture of the appropriate alkyl/phenyl 4'-fluorophenyl ketone (1 equiv, 3 mmol), the properly substituted phenol, 1-naphthol or phenylthiol (1 equiv, 3 mmol), and anhydrous potassium carbonate (1.2 equiv, 3.6 mmol) in anhydrous DMF (3 mL) was stirred at 175 °C for 5 h. After the completion of the reaction, the medium was quenched with water (50 mL) and the product was extracted with ethyl acetate (3 × 25 mL). The organic phase was washed with saturated sodium chloride (2 × 50 mL), dried over anhydrous sodium sulfate, filtered and concentrated under reduced pressure. The crude product was purified by silica gel column chromatography eluting with a mixture of ethyl acetate/*n*-hexane to obtain the pure ketones **45f-q, s-u.**

General Procedure for the Synthesis of the intermediate amines 46i-f'. A 2 M methylamine solution in methanol or, alternatively, 7 M ammonia solution in methanol (3-6 equiv, 6-12 mmol) was added to a solution of titanium *iso*propoxide (1.3-2 equiv, 2.6-4 mmol) and the carbonyl compounds **45a-w** (1 equiv, 2 mmol) in THF (5 mL), and the reaction mixture was stirred under nitrogen atmosphere at room temperature. After 5-6 h, sodium borohydride (1.1 equiv, 2.2 mmol) was added portion wise at 0 °C, and the mixture was stirred for 2 h at room temperature. After the completion, the reaction was quenched with distilled water (2 mL) and acidified at 0 °C with 1 M hydrochloric acid until pH was 1-2. The resulting suspension was filtered on celite and washed with a mixture of water (50 mL) and ethyl acetate (50 mL). The filtrate and the washings were combined, extracted with ethyl acetate (3 × 30 mL), basified with 10 % w/w sodium hydroxide up to pH 10-12 and further extracted with ethyl acetate (3 × 30 mL). The organic phase was dried over anhydrous sodium sulfate, filtered and concentrated under reduced pressure to give an oily crude product. This was finally purified by silica gel column chromatography

eluting with a mixture of chloroform/methanol/ammonia or ethyl acetate/*n*-hexane thus affording the pure amines **46i-f'**.

General Procedure for the Synthesis of the 2-Substituted 4-Aminopyrimidin-5-Carbonitriles 47a-f'. The 4-amino-2-bromopyrimidine-5-carbonitrile (1 equiv, 1 mmol) and triethylamine (1.6 equiv, 1.6 mmol) were added to a solution of the amines **46** (1 equiv, 1 mmol) in dry 2-methoxyetanol. After stirring at room temperature for 2.5 h, the reaction was stopped, and the solvent evaporated. The residue was diluted with ethyl acetate and washed two times with potassium hydrogen sulfate 0.1 N. The aqueous layer was counterextracted with ethyl acetate and the combined organic phases were dried over sodium sulfate, filtered and evaporated under reduced pressure. The crude residue was finally purified by silica gel column chromatography eluting with a mixture chloroform/*n*-hexane to afford the desired intermediate compounds **47** as white solids.

***In vitro* Antischistosomal effects of *Sm*Sirt2 inhibitors:**

Parasite material and ethics statement

A Puerto Rican strain of *Schistosoma mansoni* is maintained in the laboratory using albino *Biomphalaria glabrata* snails as intermediate host and *Mesocricetus auratus* (golden hamsters) as definitive host. Cercaria were released from infested snails and harvested on ice as described previously[65] Schistosomula were prepared *in vitro* by mechanical transformation.[65] 8 weeks post infestation, *S. mansoni* adult worms were recovered from the hamster hepatic system by whole body perfusion with saline solution pumped through a perfusing needle placed in the left ventricle of the heart.[66] All animal experimentation was conducted in accordance with the European Convention for the Protection of Vertebrate Animals used for Experimental and other Scientific Purposes (ETS No 123, revised Appendix A) and was approved by the committee for ethics in animal experimentation of the Nord-Pas de Calais region (Authorization No.

APAFIS#8289-2016122015127050V3) and the Pasteur Institute of Lille (Agreement No. B59-350009).

Schistosomula viability. 500 schistosomula were incubated at 37°C under a humid atmosphere containing 5% CO2 during 72 H in a 24-well plate containing 1 mL of complete medium (M199 medium (Invitrogen) supplemented with penicillin (50 U/mL), streptomycin (50 µg/mL), gentamycin (15 µg/mL) and rifampicin (60 µg/mL) and 10% fetal calf serum (Gibco). Parasite death was evaluate by eye examination under a microscoscpe 72 hours after the beginning of treatment using three major criteria: absence of motility, tegument defects, granular appearance. For each condition, we observed a minimum of 300 larvae in order to determine the ratio of dead larvae to total larvae. Moreover, for each condition, two different assays were perfomed and two independent batches of schistosomula (biological replicates) were used. *Sm*Sirt2 inhibitors were dissolved in DMSO and two different concentration (10 and 20 µM) were used (single dose at D0).

Adult worm pairing stability and egg laying. Ten pairs of *S. mansoni* adult worms were maintained in culture for 72 h in a 5% CO_2 atmosphere at 37°C in a 6 well-plate containing 4 mL of complete medium in the presence of *Sm*Sirt2 inhibitors at 10 and 20 µM final concentration. Every day, the number of paired couples was evaluated by eye examination. At the end of the experiement, medium containing eggs was harvested and the total number of eggs was determined after centrifugation by microscopy and two different assays were performed for each condition and repeated with two independent biological replicates.

Cell proliferation assay. HL-60 cells (grown in RPMI 1640 supplemented with 10% fetal bovine serum) were incubated in a 96 well-tissue culture plates (density of 5000 per well) with *Sm*Sirt2 inhibitors at 10 µM final concentration or DMSO vehicle as control, in a total volume of 100 µL for 72 hours at 37 °C; three replicates per concentration were used. Growth inhibition

was determined using the CellTiter 96® AQueous Non-Radioactive Cell Proliferation Assay according to the manufacturer's instructions. Data was plotted as absorbance units against compound concentration using GraphPad Prism 7.0.

References

(1) Gray, D. J.; Ross, A. G.; Li, Y. S.; McManus, D. P. Diagnosis and Management of Schistosomiasis. *Brit. Med. J.* **2011**, *342*, 1–12. https://doi.org/10.1136/bmj.d2651.

(2) Cioli, D.; Pica-Mattoccia, L.; Basso, A.; Guidi, A. Schistosomiasis Control: Praziquantel Forever? *Mol. Biochem. Parasitol.* **2014**, *195*, 23–29. https://doi.org/10.1016/j.molbiopara.2014.06.002.

(3) Fenwick, A.; Webster, J. P.; Bosque-Oliva, E.; Blair, L.; Fleming, F. M.; Zhang, Y.; Garba, A.; Stothard, J. R.; Gabrielli, A. F.; Clements, A. C. A.; et al. The Schistosomiasis Control Initiative (SCI): Rationale, Development and Implementation from 2002-2008. *Parasitology* **2009**, *136* (13), 1719–1730. https://doi.org/10.1017/S0031182009990400.

(4) Webster, J. P.; Molyneux, D. H.; Hotez, P. J.; Fenwick, A. The Contribution of Mass Drug Administration to Global Health: Past, Present and Future. *Philos. Trans. R. Soc. B Biol. Sci.* **2014**, *369*, 20130434. https://doi.org/10.1098/rstb.2013.0434.

(5) Cleland, C. R.; Tukahebwa, E. M.; Fenwick, A.; Blair, L. Mass Drug Administration with Praziquantel Reduces the Prevalence of Schistosoma {mansoni} and Improves Liver Morbidity in Untreated Preschool Children. *Trans. R. Soc. Trop. Med. Hyg.* **2014**, *108*, 575–581. https://doi.org/10.1093/trstmh/tru097.

(6) Vale, N.; Gouveia, M. J.; Rinaldi, G.; Brindley, P. J.; Gärtner, F.; Da Costa, J. M. C. Praziquantel for Schistosomiasis: Single-Drug Metabolism Revisited, Mode of Action, and Resistance. *Antimicrob. Agents Chemother.* **2017**, *61*, e02582-16. https://doi.org/10.1128/AAC.02582-16.

(7) Da Silva, V. B. R.; Campos, B. R. K. L.; De Oliveira, J. F.; Decout, J. L.; do Carmo Alves de Lima, M. Medicinal Chemistry of Antischistosomal Drugs: Praziquantel and Oxamniquine. *Bioorganic Med. Chem.* **2017**, *25*, 3259–3277.

https://doi.org/10.1016/j.bmc.2017.04.031.

(8) Siqueira, L. D. P.; Fontes, D. A. F.; Aguilera, C. S. B.; Timóteo, T. R. R.; Ângelos, M. A.; Silva, L. C. P. B. B.; de Melo, C. G.; Rolim, L. A.; da Silva, R. M. F.; Neto, P. J. R. Schistosomiasis: Drugs Used and Treatment Strategies. *Acta Trop.* **2017**, *176*, 179–187. https://doi.org/10.1016/j.actatropica.2017.08.002.

(9) Pica-Mattoccia, L.; Doenhoff, M. J.; Valle, C.; Basso, A.; Troiani, A. R.; Liberti, P.; Festucci, A.; Guidi, A.; Cioli, D. Genetic Analysis of Decreased Praziquantel Sensitivity in a Laboratory Strain of Schistosoma {mansoni}. *Acta Trop.* **2009**, *111*, 82–85. https://doi.org/10.1016/j.actatropica.2009.01.012.

(10) Pierce, R. J.; Dubois-Abdesselem, F.; Caby, S.; Trolet, J.; Lancelot, J.; Oger, F.; Bertheaume, N.; Roger, E. Chromatin Regulation in Schistosomes and Histone Modifying Enzymes as Drug Targets. *Mem. Inst. Oswaldo Cruz* **2011**, *106*, 794–801. https://doi.org/10.1590/S0074-02762011000700003.

(11) Noël, F.; Mendonça-Silva, D. L.; Thibaut, J. P. B.; Lopes, D. V. S. Characterization of Two Classes of Benzodiazepine Binding Sites in Schistosoma {mansoni}. *Parasitology* **2007**, *134*, 1003–1012. https://doi.org/10.1017/S0031182007002442.

(12) Berriman, M.; Haas, B. J.; Loverde, P. T.; Wilson, R. A.; Dillon, G. P.; Cerqueira, G. C.; Mashiyama, S. T.; Al-Lazikani, B.; Andrade, L. F.; Ashton, P. D.; et al. The Genome of the Blood Fluke Schistosoma Mansoni. *Nature* **2009**, *460*, 352–358. https://doi.org/10.1038/nature08160.

(13) Dissous, C.; Grevelding, C. G. Piggy-Backing the Concept of Cancer Drugs for Schistosomiasis Treatment: A Tangible Perspective? *Trends Parasitol.* **2011**, *27*, 59–66. https://doi.org/10.1016/j.pt.2010.09.001.

(14) Pierce, R. Targeting Schistosome Histone Modifying Enzymes for Drug Development.

Curr. Pharm. Des. **2012**, 3567–3578. https://doi.org/10.2174/138161212801327248.

(15) Arrowsmith, C. H.; Bountra, C.; Fish, P. V.; Lee, K.; Schapira, M. Epigenetic Protein Families: A New Frontier for Drug Discovery. *Nat. Rev. Drug Discov.* **2012**, *11*, 384–400. https://doi.org/10.1038/nrd3674.

(16) Wagner, J. M.; Hackanson, B.; Lübbert, M.; Jung, M. Histone Deacetylase (HDAC) Inhibitors in Recent Clinical Trials for Cancer Therapy. *Clin. Epigenetics* **2010**, *1*, 117–136. https://doi.org/10.1007/s13148-010-0012-4.

(17) Zwergel, C.; Stazi, G.; Valente, S.; Mai, A. Histone Deacetylase Inhibitors : Updated Studies in Various Epigenetic - Related Diseases. *J. Clin. Epigenetics* **2016**, *2*, 1–15. https://doi.org/10.21767/2472-1158.100015.

(18) Hailu, G.; Robaa, D.; Forgione, M.; Sippl, W.; Rotili, D.; Mai, A. Lysine Deacetylase Inhibitors in Parasites: Past, Present, and Future Perspectives. *J. Med. Chem.* **2017**, *60*, 4780–4804. https://doi.org/10.1021/acs.jmedchem.6b01595.

(19) Stolfa, D. A.; Marek, M.; Lancelot, J.; Hauser, A. T.; Walter, A.; Leproult, E.; Melesina, J.; Rumpf, T.; Wurtz, J. M.; Cavarelli, J.; et al. Molecular Basis for the Antiparasitic Activity of a Mercaptoacetamide Derivative That Inhibits Histone Deacetylase 8 (HDAC8) from the Human Pathogen Schistosoma {mansoni}. *J. Mol. Biol.* **2014**, *426*, 3442–3453. https://doi.org/10.1016/j.jmb.2014.03.007.

(20) Simoben, C. V.; Robaa, D.; Chakrabarti, A.; Schmidtkunz, K.; Marek, M.; Lancelot, J.; Kannan, S.; Melesina, J.; Shaik, T. B.; Pierce, R. J.; et al. A Novel Class of Schistosoma {mansoni} Histone Deacetylase 8 (HDAC8) Inhibitors Identified by Structure-Based Virtual Screening and in Vitro Testing. *Molecules* **2018**, *23*, 1–14. https://doi.org/10.3390/molecules23030566.

(21) Heimburg, T.; Chakrabarti, A.; Lancelot, J.; Marek, M.; Melesina, J.; Hauser, A. T.; Shaik,

T. B.; Duclaud, S.; Robaa, D.; Erdmann, F.; et al. Structure-Based Design and Synthesis of Novel Inhibitors Targeting HDAC8 from Schistosoma {mansoni} for the Treatment of Schistosomiasis. *J. Med. Chem.* **2016**, *59*, 2423–2435. https://doi.org/10.1021/acs.jmedchem.5b01478.

(22) Peck, B.; Chen, C. Y.; Ho, K. K.; Di Fruscia, P.; Myatt, S. S.; Coombes, R. C.; Fuchter, M. J.; Hsiao, C. D.; Lam, E. W. F. SIRT Inhibitors Induce Cell Death and p53 Acetylation through Targeting Both SIRT1 and SIRT2. *Mol. Cancer Ther.* **2010**, *9*, 844–855. https://doi.org/10.1158/1535-7163.MCT-09-0971.

(23) Chakrabarty, S. P.; Saikumari, Y. K.; Bopanna, M. P.; Balaram, H. Biochemical Characterization of Plasmodium Falciparum Sir2, a NAD+-Dependent Deacetylase. *Mol. Biochem. Parasitol.* **2008**, *158* (2), 139–151. https://doi.org/10.1016/j.molbiopara.2007.12.003.

(24) Tonkin, C. J.; Carret, C. K.; Duraisingh, M. T.; Voss, T. S.; Ralph, S. A.; Hommel, M.; Duffy, M. F.; Da Silva, L. M.; Scherf, A.; Ivens, A.; et al. Sir2 Paralogues Cooperate to Regulate Virulence Genes and Antigenic Variation in Plasmodium Falciparum. *PLoS Biol.* **2009**, *7* (4), 0771–0788. https://doi.org/10.1371/journal.pbio.1000084.

(25) Moretti, N. S.; Augusto, L. D. S.; Clemente, T. M.; Antunes, R. P. P.; Yoshida, N.; Torrecilhas, A. C.; Cano, M. I. N.; Schenkman, S. Characterization of Trypanosoma {cruzi} Sirtuins as Possible Drug Targets for Chagas Disease. *Antimicrob. Agents Chemother.* **2015**, *59*, 4669–4679. https://doi.org/10.1128/AAC.04694-14.

(26) Ritagliati, C.; Alonso, V. L.; Manarin, R.; Cribb, P.; Serra, E. C. Overexpression of Cytoplasmic TcSIR2RP1 and Mitochondrial TcSIR2RP3 Impacts on Trypanosoma {cruzi} Growth and Cell Invasion. *PLoS Negl. Trop. Dis.* **2015**, *9*, 1–22. https://doi.org/10.1371/journal.pntd.0003725.

(27) Yahiaoui, B.; Taibi, A.; Ouaissi, A. A Leishmania Major Protein with Extensive Homology to Silent Information Regulator 2 of Saccharomyces {cerevisiae}. *Gene* **1996**, *169*, 115–118. https://doi.org/10.1016/0378-1119(95)00785-7.

(28) Vergnes, B.; Sereno, D.; Madjidian-Sereno, N.; Lemesre, J. L.; Ouaissi, A. Cytoplasmic SIR2 Homologue Overexpression Promotes Survival of Leishmania Parasites by Preventing Programmed Cell Death. *Gene* **2002**, *296*, 139–150. https://doi.org/10.1016/S0378-1119(02)00842-9.

(29) Tavares, J.; Ouaissi, A.; Silva, A. M.; Lin, P. K. T.; Roy, N.; Cordeiro-da-Silva, A. Anti-Leishmanial Activity of the Bisnaphthalimidopropyl Derivatives. *Parasitol. Int.* **2012**, *61*, 360–363. https://doi.org/10.1016/j.parint.2011.11.005.

(30) Lancelot, J.; Caby, S.; Dubois-Abdesselem, F.; Vanderstraete, M.; Trolet, J.; Oliveira, G.; Bracher, F.; Jung, M.; Pierce, R. J. Schistosoma {mansoni} Sirtuins: Characterization and Potential as Chemotherapeutic Targets. *PLoS Negl. Trop. Dis.* **2013**, *7*, 1–13. https://doi.org/10.1371/journal.pntd.0002428.

(31) Grozinger, C. M.; Chao, E. D.; Blackwell, H. E.; Moazed, D.; Schreiber, S. L. Identification of a Class of Small Molecule Inhibitors of the Sirtuin Family of NAD-Dependent Deacetylases by Phenotypic Screening. *J. Biol. Chem.* **2001**, *276*, 38837–38843. https://doi.org/10.1074/jbc.M106779200.

(32) Lara, E.; Mai, A.; Calvanese, V.; Altucci, L.; Lopez-Nieva, P.; Martinez-Chantar, M. L.; Varela-Rey, M.; Rotili, D.; Nebbioso, A.; Ropero, S.; et al. Salermide, a Sirtuin Inhibitor with a Strong Cancer-Specific Proapoptotic Effect. *Oncogene* **2009**, *28*, 781–791. https://doi.org/10.1038/onc.2008.436.

(33) Rotili, D.; Tarantino, D.; Nebbioso, A.; Paolini, C.; Huidobro, C.; Lara, E.; Mellini, P.; Lenoci, A.; Pezzi, R.; Botta, G.; et al. Discovery of Salermide-Related Sirtuin Inhibitors:

Binding Mode Studies and Antiproliferative Effects in Cancer Cells Including Cancer Stem Cells. *J. Med. Chem.* **2012**, *55* (24), 10937–10947. https://doi.org/10.1021/jm3011614.

(34) Wang, J.; Kim, T. H.; Ahn, M. Y.; Lee, J.; Jung, J. H.; Choi, W. S.; Lee, B. M.; Yoon, K. S.; Yoon, S.; Kim, H. S. Sirtinol, a Class III HDAC Inhibitor, Induces Apoptotic and Autophagic Cell Death in MCF-7 Human Breast Cancer Cells. *Int. J. Oncol.* **2012**, *41*, 1101–1109. https://doi.org/10.3892/ijo.2012.1534.

(35) Pasco, M. Y.; Rotili, D.; Altucci, L.; Farina, F.; Rouleau, G. A.; Mai, A.; Néri, C. Characterization of Sirtuin Inhibitors in Nematodes Expressing a Muscular Dystrophy Protein Reveals Muscle Cell and Behavioral Protection by Specific Sirtinol Analogues. *J. Med. Chem.* **2010**, *53* (3), 1407–1411. https://doi.org/10.1021/jm9013345.

(36) Du, J.; Zhou, Y.; Su, X.; Yu, J. J.; Khan, S.; Jiang, H.; Kim, J.; Woo, J.; Kim, J. H.; Choi, B. H.; et al. Sirt5 Is a NAD-Dependent Protein Lysine Demalonylase and Desuccinylase. *Science (80-.).* **2011**, *334* (6057), 806–809. https://doi.org/10.1126/science.1207861.

(37) Feldman, J. L.; Dittenhafer-Reed, K. E.; Kudo, N.; Thelen, J. N.; Ito, A.; Yoshida, M.; Denu, J. M. Kinetic and Structural Basis for Acyl-Group Selectivity and NAD + Dependence in Sirtuin-Catalyzed Deacylation. *Biochemistry* **2015**, *54*, 3037–3050. https://doi.org/10.1021/acs.biochem.5b00150.

(38) Jiang, H.; Khan, S.; Wang, Y.; Charron, G.; He, B.; Sebastian, C.; Du, J.; Kim, R.; Ge, E.; Mostoslavsky, R.; et al. SIRT6 Regulates TNF-α Secretion through Hydrolysis of Long-Chain Fatty Acyl Lysine. *Nature* **2013**, *496*, 110–113. https://doi.org/10.1038/nature12038.

(39) Olsen, C. A. An Update on Lysine Deacylases Targeting the Expanding "acylome." *ChemMedChem* **2014**, *9*, 434–437. https://doi.org/10.1002/cmdc.201300421.

(40) Bao, X.; Wang, Y.; Li, X.; Li, X. M.; Liu, Z.; Yang, T.; Wong, C. F. a.; Zhang, J.; Hao, Q.; Li, X. D. avi. Identification of "Erasers" for Lysine Crotonylated Histone Marks Using a Chemical Proteomics Approach. *Elife* **2014**, *3*, 1–18. https://doi.org/10.7554/eLife.02999.

(41) Du, J.; Zhou, Y.; Su, X.; Yu, J. J.; Khan, S.; Jiang, H.; Kim, J. H.; Woo, J.; Kim, J. H.; Choi, B. H.; et al. Sirt5 Is a NAD-Dependent Protein Lysine Demalonylase and Desuccinylase. *Science (80-.).* **2011**, *334* (November), 806–809. https://doi.org/10.1126/science.1207861.

(42) Tan, M.; Peng, C.; Anderson, K. A.; Chhoy, P.; Xie, Z.; Dai, L.; Park, J.; Chen, Y.; Huang, H.; Zhang, Y.; et al. Lysine Glutarylation Is a Protein Posttranslational Modification Regulated by SIRT5. *Cell Metab.* **2014**, *19*, 605–617. https://doi.org/10.1016/j.cmet.2014.03.014.

(43) Anderson, K. A.; Huynh, F. K.; Fisher-Wellman, K.; Stuart, J. D.; Peterson, B. S.; Douros, J. D.; Wagner, G. R.; Thompson, J. W.; Madsen, A. S.; Green, M. F.; et al. SIRT4 Is a Lysine Deacylase That Controls Leucine Metabolism and Insulin Secretion. *Cell Metab.* **2017**, *25*, 838–855. https://doi.org/10.1016/j.cmet.2017.03.003.

(44) Lin, H.; Su, X.; He, B. Protein Lysine Acylation and Cysteine Succination by Intermediates of Energy Metabolism. *Chem. Biol.* **2012**, *7*, 947–960. https://doi.org/10.1021/cb3001793.

(45) Feldman, J. L.; Baeza, J.; Denu, J. M. Activation of the Protein Deacetylase SIRT6 by Long-Chain Fatty Acids and Widespread Deacylation by Mammalian Sirtuins. *J. Biol. Chem.* **2013**, *288*, 31350–31356. https://doi.org/10.1074/jbc.C113.511261.

(46) Zhu A. Y., Zhou Y., Kahn S., Deitsch K. W., Hao Q., L. H. *Plasmodium Falciparum* Sir2A Preferentially Hydrolyzes Medium and Long Chain Fatty Acyl Lysine. *Chem. Biol.* **2012**, *7*, 155–159. https://doi.org/10.1007/s10439-011-0452-9.Engineering.

(47) Schiedel, M.; Marek, M.; Lancelot, J.; Karaman, B.; Almlöf, I.; Schultz, J.; Sippl, W.; Pierce, R. J.; Romier, C.; Jung, M. Fluorescence-Based Screening Assays for the NAD + -Dependent Histone Deacetylase smSirt2 from Schistosoma Mansoni. *J. Biomol. Screen.* **2015**, *20*, 112–121. https://doi.org/10.1177/1087057114555307.

(48) Peña, I.; Pilar Manzano, M.; Cantizani, J.; Kessler, A.; Alonso-Padilla, J.; Bardera, A. I.; Alvarez, E.; Colmenarejo, G.; Cotillo, I.; Roquero, I.; et al. New Compound Sets Identified from High Throughput Phenotypic Screening against Three Kinetoplastid Parasites: An Open Resource. *Sci. Rep.* **2015**, *5*, 8771. https://doi.org/10.1038/srep08771.

(49) Roquis, D.; Lepesant, J. M. J.; Picard, M. A. L.; Freitag, M.; Parrinello, H.; Groth, M.; Emans, R.; Cosseau, C.; Grunau, C. The Epigenome of Schistosoma Mansoni Provides Insight about How Cercariae Poise Transcription until Infection. *PLoS Negl. Trop. Dis.* **2015**, *9* (8), 1–22. https://doi.org/10.1371/journal.pntd.0003853.

(50) Heltweg, B.; Trapp, J.; Jung, M. In Vitro Assays for the Determination of Histone Deacetylase Activity. *Methods* **2005**, *36*, 332–337. https://doi.org/10.1016/j.ymeth.2005.03.003.

(51) Sauve, A. A.; Youn, D. Y. Sirtuins : NAD + -Dependent Deacetylase Mechanism and Regulation. *Curr. Opin. Chem. Biol.* **2012**, *16*, 535–543. https://doi.org/10.1016/j.cbpa.2012.10.003.

(52) Borra, M. T.; Langer, M. R.; Slama, J. T.; Denu, J. M. Substrate Specificity and Kinetic Mechanism of the Sir2 Family of NAD+-Dependent Histone/protein Deacetylases. *Biochemistry* **2004**, *43* (30), 9877–9887. https://doi.org/10.1021/bi049592e.

(53) Rumpf, T.; Schiedel, M.; Karaman, B.; Roessler, C.; North, B. J.; Lehotzky, A.; Ova'di, J.; Ladwein, K. I.; Schmidtkunz, K.; Gajer, M.; et al. [PDB ID: 4RMG] Selective Sirt2 Inhibition by Ligand-Induced Rearrangement of the Active Site. *Nat. Commun.* **2015**, *6*,

6263. https://doi.org/10.1038/ncomms7263.

(54) Hoffmann, G.; Breitenbücher, F.; Schuler, M.; Ehrenhofer-Murray, A. E. A Novel Sirtuin 2 (SIRT2) Inhibitor with p53-Dependent pro-Apoptotic Activity in Non-Small Cell Lung Cancer. *J. Biol. Chem.* **2014**, *289* (8), 5208–5216. https://doi.org/10.1074/jbc.M113.487736.

(55) Swyter, S.; Schiedel, M.; Monaldi, D.; Sippl, W.; Lehotzky, A.; Rumpf, T.; Ovadi, J.; Jung, M. New Chemical Tools for Probing Activity and Inhibition of the NAD+ - Dependent Lysine Deacylase Sirtuin 2. *Phil. Trans. R. Soc.* **2018**, *373*, 20170083.

(56) Schiedel, M.; Marek, M.; Lancelot, J.; Karaman, B.; Almlöf, I.; Schultz, J.; Sippl, W.; Pierce, R. J.; Romier, C.; Jung, M. Fluorescence-Based Screening Assays for the NAD^+ - Dependent Histone Deacetylase smSirt2 from *Schistosoma Mansoni*. *J. Biomol. Screen.* **2015**, *20* (1), 112–121. https://doi.org/10.1177/1087057114555307.

(57) Panic, G.; Vargas, M.; Scandale, I.; Keiser, J. Activity Profile of an FDA-Approved Compound Library against Schistosoma Mansoni. *PLoS Negl. Trop. Dis.* **2015**, *9*, 1–15. https://doi.org/10.1371/journal.pntd.0003962.

(58) Abdulla, M. H.; Ruelas, D. S.; Wolff, B.; Snedecor, J.; Lim, K. C.; Xu, F.; Renslo, A. R.; Williams, J.; McKerrow, J. H.; Caffrey, C. R. Drug Discovery for Schistosomiasis: Hit and Lead Compounds Identified in a Library of Known Drugs by Medium-Throughput Phenotypic Screening. *PLoS Negl. Trop. Dis.* **2009**, *3*, e478. https://doi.org/10.1371/journal.pntd.0000478.

(59) Schiedel, M.; Rumpf, T.; Karaman, B.; Lehotzky, A.; Oláh, J.; Gerhardt, S.; Ovádi, J.; Sippl, W.; Einsle, O.; Jung, M. Aminothiazoles as Potent and Selective Sirt2 Inhibitors: A Structure-Activity Relationship Study. *J. Med. Chem.* **2016**, *59* (4), 1599–1612. https://doi.org/10.1021/acs.jmedchem.5b01517.

(60) Green, B. T.; Lee, S. T.; Welch, K. D.; Panter, K. E. Plant Alkaloids That Cause Developmental Defects through the Disruption of Cholinergic Neurotransmission. *Birth Defects Res. Part C - Embryo Today Rev.* **2013**, *99*, 235–246. https://doi.org/10.1002/bdrc.21049.

(61) Barradas, S.; Hern, G.; Urbano, A.; Carre, M. C. Total Synthesis of Natural P - Quinol Cochinchinenone. *Org. Lett.* **2012**, *14* (23), 5952–5955.

(62) Biscoe, M. R.; Fors, B. P.; Buchwald, S. L. A New Class of Easily Activated Palladium Precatalysts for Facile C - N Cross-Coupling Reactions and the Low Temperature Oxidative Addition of Aryl Chlorides. *J. Am. Chem. Soc.* **2008**, *130*, 6686–6687.

(63) Vicker, N.; Xiangdong, S.; Ganeshapillai, D.; Purhoit, A.; Reed, M. J.; Potter, B. WO2005042513A1. 2005.

(64) Spiegelman, N. A.; Price, I. R.; Jing, H.; Wang, M.; Yang, M.; Cao, J.; Hong, J. Y.; Zhang, X.; Aramsangtienchai, P.; Sadhukhan, S.; et al. Direct Comparison of SIRT2 Inhibitors: Potency, Specificity, Activity-Dependent Inhibition, and On-Target Anticancer Activities. *ChemMedChem* **2018**, 1–6. https://doi.org/10.1002/cmdc.201800391.

(65) Ramalho-Pinto, F. J.; Gazzinelli, G.; Howells, R. E.; Mota-Santos, T. A.; Figueiredo, E. A.; Pellegrino, J. Schistosoma Mansoni: Defined System for Stepwise Transformation of Cercaria to Schistosomule in Vitro. *Exp. Parasitol.* **1974**, *36* (3), 360–372. https://doi.org/10.1016/0014-4894(74)90076-9.

(66) Smithers, S. R.; Terry, R. J. The Infection of Laboratory Hosts with Cercariae of Schistosoma Mansoni and the Recovery of the Adult Worms. *Parasitology* **1965**, *55* (4), 695–700. https://doi.org/10.1017/S0031182000086248.

Table of Contents graphic